

Debiasing Large Visual Language Models

Yi-Fan Zhang¹, Weichen Yu², Qingsong Wen³ ^{*}, Xue Wang⁴, Zhang Zhang¹,
Liang Wang¹, Rong Jin⁵, and Tieniu Tan¹

¹ State Key Laboratory of Multimodal Artificial Intelligence Systems (MAIS),
Institute of Automation

² Carnegie Mellon University

³ Squirrel AI Learning, ^{*} Corresponding author

⁴ Alibaba Group

⁵ Meta AI

<https://github.com/yfzhang114/LLaVA-Align>

Abstract. In the realms of computer vision and natural language processing, Large Vision-Language Models (LVLMs) have become indispensable tools, proficient in generating textual descriptions based on visual inputs. Despite their advancements, our investigation reveals a noteworthy bias in the generated content, where the output is primarily influenced by the underlying Large Language Models (LLMs) prior rather than the input image. Our empirical experiments underscore the persistence of this bias, as LVLMs often provide confident answers even in the absence of relevant images or given incongruent visual input. To rectify these biases and redirect the model’s focus toward vision information, we introduce two simple, training-free strategies. Firstly, for tasks such as classification or multi-choice question-answering (QA), we propose a “calibration” step through affine transformation to adjust the output distribution. This “Post-Hoc debias” approach ensures uniform scores for each answer when the image is absent, serving as an effective regularization technique to alleviate the influence of LLM priors. For more intricate open-ended generation tasks, we extend this method to “Debias sampling”, drawing inspirations from contrastive decoding methods. Furthermore, our investigation sheds light on the instability of LVLMs across various decoding configurations. Through systematic exploration of different settings, we significantly enhance performance, surpassing reported results and raising concerns about the fairness of existing evaluations. Comprehensive experiments substantiate the effectiveness of our proposed strategies in mitigating biases. These strategies not only prove beneficial in minimizing hallucinations but also contribute to the generation of more helpful and precise illustrations.

Keywords: Large Vision-Language Models · Debiasing · Hallucination

1 Introduction

LLMs such as GPT-4 [34], PaLM [7], and LLaMA-2 [47] have evolved to handle both text and images. This expansion into the multimodal domain involves further pre-training with image-text pairs or fine-tuning with specialized vision

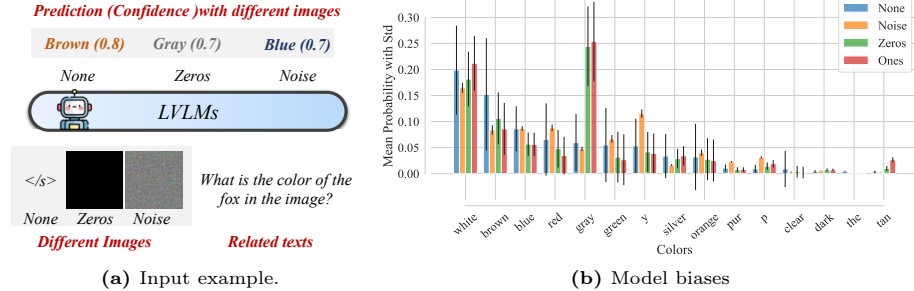


Fig. 1: LLaVA-v1.5-7B [30] generates confident answers with meaningless images. “None” indicates the absence of an input image, while “Noise” signifies the presence of Gaussian noise matching the image dimensions. “Zeros/Ones” indicates a scenario where a tensor with all zero/one values.

instruction tuning datasets, resulting in the birth of powerful Large Visual Language Models (LVLMs). These models excel at understanding complex visual patterns and translating them into coherent language. However, despite their capabilities, our investigation reveals a notable issue. The content generated by LVLMs is significantly biased towards the underlying LLMs used during pre-training, rather than being influenced by the input images. Even in situations where the image is entirely noisy or absent, LVLMs confidently generate answers, indicating a bias towards the learned language patterns. This observation is illustrated in Fig. 1, where querying an LVLM about the color of a non-existent fox produces confident yet unrealistic answers like brown, gray, or blue. To explore this bias further, we conduct a toy experiment using questions about color, shape, number, and relationships for 80 entities in the MSCOCO dataset. Our experimental baselines include **Noise** (fully noisy image and question input), **None** (no image provided), and **Zeros/Ones** (image with all zero/one values). Fig. 1 displays the top 15 choices and corresponding probabilities of frequently occurring answers across these cases. Remarkably, even when no image is available or questions are about non-existent or meaningless images, current LVLMs tend to produce specific answers. This indicates a substantial bias originating from the pretraining on LLMs. Such biases bring persistent challenges, particularly the issue of hallucination [13, 26, 26, 43], pose a significant concern, impacting the reliability and applicability of LVLMs. In this paper, we also aim to uncover the underlying reasons behind such a phenomenon, and the results will provide insights into the design of current LVLMs and their training strategies.

In this paper, we present two training-free strategies to mitigate generation biases associated with underlying LLMs. Our first approach introduces a “calibration” step to adjust the output distribution. Specifically, we assess the model’s inclination toward specific answers by inputting a dummy test with no image, as illustrated in Fig. 1, where we replace the image with ‘None’ or meaningless tensors. We then determine the calibration parameters to ensure that the image-free input produces uniform scores for each answer without yielding overly confident outputs. This calibration procedure establishes suitable param-

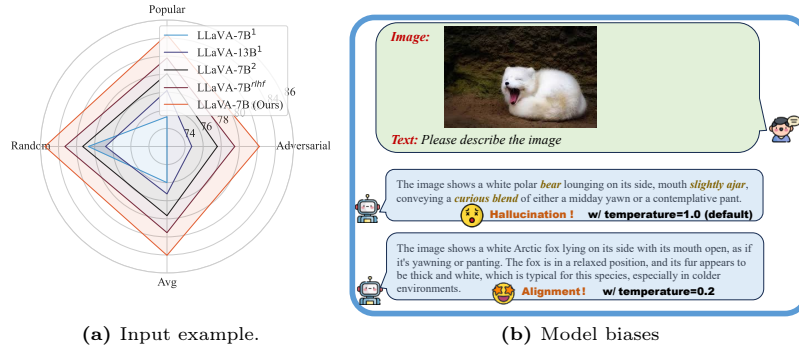


Fig. 2: Leveraging diverse generation strategies improves the overall truthfulness score. The superscripts 1 and 2 reference outcomes from distinct paper reports [21, 43], where “rlhf” signifies models fine-tuned using the RLHF technique [43]. In this instance, a simple adjustment of the temperature from the default 1.0 to 0.2 is demonstrated, resulting in the successful generation of aligned output.

eters without requiring additional training data, referred to as the “**Post-Hoc debias**” approach, proving intuitive for classification tasks⁶. However, in open-ended generation, calibrating each token’s logits uniformly, even without image input, is unreasonable due to the inherent correlation between text tokens. In such cases, we extend the Post-Hoc debias method to its “**Debias sampling**” counterpart. Inspired by contrastive decoding methods [21, 25], we compute the difference between generation token log-probabilities for one with a correct image and another with a meaningless vision input. Both the Post-Hoc debias and debias sampling methods serve as regularization techniques, reducing the generation results’ dependency on pure text or meaningless image input.

Moreover, we have identified a significant level of instability in the performance of current LVLMs across various generative configurations. Our primary hypothesis is that existing evaluations are predominantly based on a default decoding setting, limiting the exploration of the model’s full capabilities. As extensively illustrated in Fig. 2, diverse choices in generative configurations yield substantially different performance outcomes. Notably, adjusting the generation temperature can lead to a notable increase in the average F1 score of POPE-MSCOCO, shifting from 76 to approximately 84.04. This improvement surpasses the previous results achieved by the 13B model and the RLHF-tuned model by a considerable margin, indicating that the current estimation of LVLM capability may be underestimated. Furthermore, our investigation reveals that different models exhibit preferences for distinct generation configurations, highlighting the instability in the current evaluation of LVLMs. This raises concerns about the fairness of evaluations, particularly since they often rely on default generation configurations or selectively choose the best configuration for the proposed model. To maximize the full potential of existing LVLMs, we systematically in-

⁶ In binary classification settings like POPE, we aim for the input with a meaningless image to have ‘yes’ and ‘no’ with an equal probability of 50%.

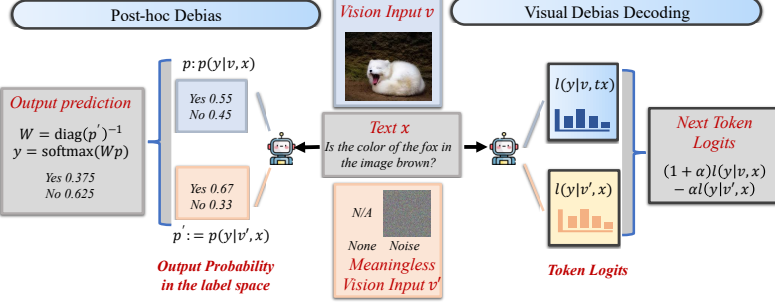


Fig. 3: Illustration of the proposed Post-hoc debiasing and debias sampling methods. The former focuses on debiasing the prediction results, while the latter modifies the generation distribution of the next token.

vestigate six LVLM models across four benchmarks, meticulously searching their generative configurations to identify optimal settings. Our results significantly outperform previously reported ones by a substantial margin, underscoring the importance of selecting the best decoding configuration for each model.

2 Method

Background of Large Vision-Language Models. A LVLM with parameters θ , conditioned on a query text $x := (x_1, \dots, x_m)$, a vision input v , parametrizes a probability distribution over response sequences $y := (y_1, \dots, y_n)$. Each response token is sampled from a token probability distribution, namely $y_t \sim p_\theta(y_t|x, v, y_{<t}) \propto \exp l_\theta(y_t|x, v, y_{<t})$, where $l_\theta(y_t|\cdot)$ denotes the logits of y_t . Usually, an LLM is first pre-trained on a large, unlabeled text dataset, then an LVLM utilizes the LLM as the text encoder and incorporates vision representations in different ways [3, 9, 12, 23]. Related work about LVLMs and Hallucination in LVLMs can be found in Appendix A.

2.1 Exploring the Impact of LLM Biases on LVLMs

Addressing Biases in Current LVLMs. Despite the acknowledged influence of language priors on VQA tasks [15, 53, 57], previous efforts have primarily concentrated on mitigating biases within the training sets. These approaches involve designing advanced training strategies and constructing balanced datasets. However, extending such methods to LVLMs, which utilize pre-existing LLMs as text encoders, is challenging due to the complexity and cost associated with retraining or fine-tuning. Furthermore, it remains unclear whether LVLM performance is affected by the language priors ingrained in their used LLMs.

To assess the influence of LLM biases on LVLMs, we conduct toy experiments with five target questions detailed in Tab. 4. For each entity of the MSCOCO dataset (appendix Tab. 3), we design corresponding prompts and pair them with different types of vision inputs, including **unrelated vision input** such as fully noisy images (Noise) or entirely black or white images (Zero/One), or **replace vision input with pure text**, where we either remove all vision

tokens (None) or replace them with a meaningless placeholder like `</unk>` (Unk). As illustrated in Fig. 1 and in the appendix Fig. 13, LVLMs exhibit biases towards specific answers, such as associating “white” with color-related questions, “round” with shape-related questions, and “many” with number-based questions. We further analyze attention mechanisms to explain why models heavily rely on LLM biases. Fig. 4 and 14 demonstrate that LLM outputs tend to allocate more attention to text tokens. Even for original image-text pairs where the number of image tokens exceeds that of text tokens, the sum of attention scores for text surpasses 90%. An intriguing observation is that when we feed the original text-image pair (Naive), pure text (None), and fully noisy images (Noise), the model exhibits similar attention patterns. Most attention is directed towards special but uninformative tokens, rather than vision tokens or text sequences, such as the question itself. **In open-ended generation tasks**, we randomly select two questions from LLaVA-Bench (as shown in Fig. 11) and examine the attention scores as more tokens were generated. As depicted in Fig. 5, with the increasing length of generated text during open-ended tasks, there was a corresponding reduction in attention allocated to images, exacerbating the issue. Consequently, the model becomes increasingly prone to generating content independently of input images, shedding light on the genesis of hallucinated content from an attention perspective. Additionally, the results also indicate that the shallow layers assign higher attention to visual tokens; however, as the feature progresses into deeper layers, attention on vision tokens will be reduced.

Underlying Reasons: Several factors contribute to the existence of this phenomenon, with the modality gap [27] standing out as a pivotal influencer. This gap becomes apparent as image-text embeddings consistently reside in distinct spaces with substantial distances, a characteristic observed even in models trained on a significant number of image-text pairs [37]. Unfortunately, LVLMs consistently undergo training with a restricted vision-language dataset [43], resulting in a weakened feature alignment. In contrast, the LLMs involved in the process benefit from a more extensive training corpus and demonstrate heightened proficiency in addressing *text-based tasks*. The pronounced modality gap guides LLMs to predominantly focus on familiar tokens or representations, often neglecting crucial vision tokens. Additionally, following the *shallow-to-deep principle* [35, 39], where shallower networks can adeptly adapt to changes in data streams or learn more efficiently with limited data, we can explain why shallow layers exhibit better attention score assignments compared to deeper layers. Shallow layers may be better tuned, but deeper layers retain most of the original LLM patterns and tend to ignore unfamiliar vision tokens. Furthermore, LVLMs may inherit the drawbacks of LLMs, which often overlook contextual information and heavily rely on their prior parametric knowledge [5, 42, 54], further diminishing the impact of vision tokens. These revelations underscore inherent limitations in current training strategies and datasets, emphasizing the need for enhanced alignment between the two modalities or a heightened recognition of the contribution made by vision tokens. In response to this challenge, we present

a series of training-free methods in this paper, with the aim of mitigating the observed phenomenon and elevating the overall performance of LVLMs.

2.2 Model Calibration

Post-hoc Debiasing of Prediction Results (Fig. 3 (left)). In addressing the bias issue, we implement a “calibration” step for the model’s output probabilities using an affine transformation [14, 36, 52]: $y = \text{softmax}(Wp_\theta + b)$. In this equation, a weight matrix W and a bias vector b are applied to the original probabilities, producing adjusted probabilities. For classification tasks, p represents the probabilities associated with each label name, normalized to sum up to one. To enhance efficiency, we constrain the matrix W to be diagonal, utilizing vector scaling [14, 52]. An intuitive approach to learning W is to initially estimate the LLM’s bias towards certain answers by inputting a meaningless vision input v' , such as None or Noise. The resulting output prediction is denoted as $p' := p'_\theta(y|x, v')$. Ideally, LLMs should assign a uniform distribution score to this test input. For instance, when presented with the question “*Is the color of the fox in the image brown?*”, supplying a meaningless image or no image should result in equal probabilities for ‘yes’ and ‘no’. This is because the model cannot make a decision. However, due to the model’s biases, it tends to assign a higher score to ‘yes’. This error can be corrected by setting $W = \text{diag}(p'_\theta)^{-1}$ and b to an all-zero vector. Subsequently, the debiased result is obtained as $y = \text{softmax}(Wp_\theta + b)$. In our experimental findings, we establish that employing unrelated vision inputs (Noise, Zero, One) does not consistently enhance model performance and exhibits sensitivity to question types. Consequently, as a default debiasing approach, we opt for image-free methods, specifically **None** and **Unk**. Additionally, we explore a debiasing method using **Both** image-free inputs. In this configuration, we set v' to None and $</unk>$, obtaining respective probability distributions p'_n and p'_u . We then calculate the probability distribution $p' = (p'_n + p'_u)/2$.

Visual Debias Decoding (VDD) (Fig. 3 (Right)). While post-hoc debias methods can be naturally extended to open-ended generation settings with the entire vocabulary as the label space, implementation faces challenges due to the large label space. At the same time, it’s crucial to maintain the correlation or co-occurrence of output text tokens and simply enforcing a uniform LM output distribution could significantly harm generation quality. In response, we adopt the concept of contrastive decoding [21, 25, 42, 50] and introduce the VDD strategy. Similar to post-hoc debiasing, we feed the original image and text into the LVLM to obtain logits $l := l_\theta(y|x, v)$ and feed image-free input to get logits $l' := l_\theta(y|x, v')$, where l' contains only text priors. To emphasize the contribution of visual information, we aim to mitigate undesired behaviors highlighted by the image-free logits and generate text based on the remaining positive behaviors of the LVLM when provided with the image input. To implement this concept, we propose the contrastive objective: $p_{vdd}(y|v, v', x) = \text{softmax}[(1 + \alpha)l_\theta(y|x, v) - \alpha l_\theta(y|x, v')]$. In this context, α represents the amplification level of the debiasing method. It is crucial to recognize that the logits from pure-text models are not invariably incorrect. They

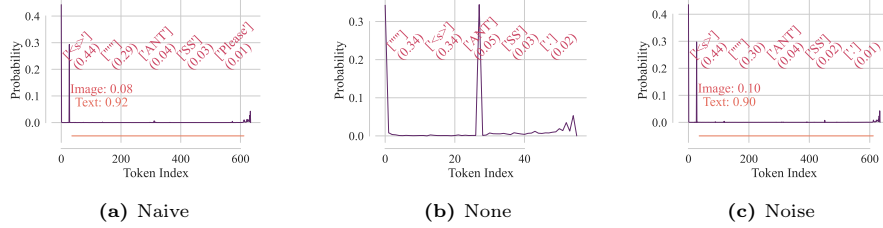


Fig. 4: Attention maps for different input images. The question is *A chat between a curious human and an artificial intelligence assistant. The assistant gives helpful, detailed, and polite answers to the human’s questions. USER: <image> Is there a bed in the image? Please answer this question with one word. ASSISTANT:*

can adeptly capture various fundamental aspects of English grammar and common sense. Therefore, adopting a universal penalty for all tokens may not be suitable in every instance. To tackle this nuanced challenge, we introduce an adaptive plausibility constraint across the output vocabulary \mathcal{V} of LVLMs. This constraint is intricately linked to the confidence level associated with the output distribution when original visual inputs are considered: $\mathcal{V}_{head}(y_t) = \{y_i \in \mathcal{V} : p_\theta(y_i|v, t, y_{<t}) \geq \beta \max_{w \in \mathcal{V}} p_\theta(w|v, t, y_{<t})\}$. Here, $\beta \in [0, 1]$ is a hyperparameter that truncates the next token distribution of p_θ . A larger β entails more aggressive truncation, keeping only high probability tokens. During generation, we set the logits of all tokens not in \mathcal{V}_{head} to $-\infty$:

$$p_{vdd}(y_t) = \text{softmax} [(1 + \alpha)l_\theta(y|x, v) - \alpha l_\theta(y|x, v')] \text{ if } y_t \in \mathcal{V}_{head}; \text{ Otherwise } 0$$

The adaptive plausibility constraint adeptly reserves high-probability tokens considering vision information, mitigating bias through the utilization of pure-text logits. This constraint maintains as few as one token in the candidate pool when the expert exhibits high confidence in a specific token, effectively mitigating the influence of the contrastive objective. Importantly, our VDD approach only necessitates the input of pure text into LVLMs, enhancing efficiency compared to visual contrastive decoding [32]. This avoids the intricacies of VCD associated with employing a distorted image to generate reference logits, a process that requires meticulous adjustment of the injected noise level into the image. Similar to post-hoc debiasing methods, here we denote the methods as VDD-None, VDD-Unk, and VDD-Both, corresponding to the use of image-free inputs None, Unk, and both for obtaining reference logits.

2.3 Impact of Decoding Configuration on Model Performance

We observe that existing open-source LVLMs undergo evaluations using a variety of generation strategies, as outlined in Tab. 5. This variability in evaluation configuration introduces a potential source of performance variability, impacting the thorough exploration of LVLM capabilities. Our research primarily delves into decoding configurations, specifically experimenting with distinct strategies:

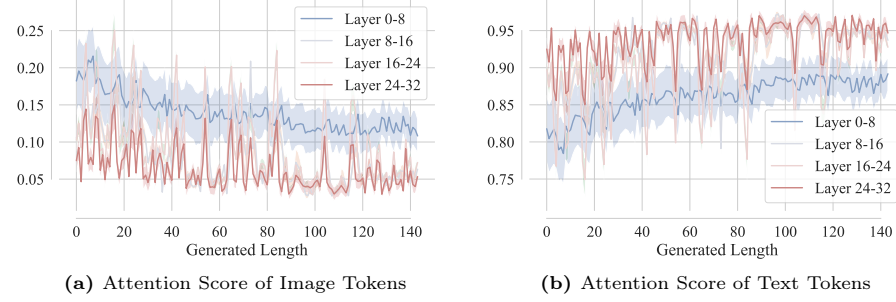


Fig. 5: Attention scores attained by each layer during generation.

1. Temperature Sampling: We systematically vary the temperature parameter (τ) from 0.05 to 1, with a step size of 0.05, resulting in 20 configurations. The temperature parameter modulates the sharpness of the next-token distribution.
2. Top- k Sampling: By filtering the K most likely next words, where K varies within 1, 2, 5, 10, 20, 50, 100, 200, 500, we generate 9 configurations.
3. Top- p Sampling: We select words from the smallest set whose cumulative probability exceeds the threshold p . The threshold p ranges from 0.05 to 1, with a step size of 0.05, yielding 20 configurations.

For each test sample of a given benchmark, the model generates 49 responses, corresponding to each decoding configuration. In the experimental section, we establish four settings: **Temp τ** , **Top- p** , and **Top- k** , where the best response for each test sample is selected among configurations within these three settings. Finally, the **Overall** setting chooses the best response from all 49 generated responses for each test sample. This systematic exploration of decoding strategies contributes to a more comprehensive understanding of LVLM performance.

3 Experiments

We conduct a series of extensive experiments to demonstrate that: (i) the proposed debiasing methods significantly alleviate hallucination and improve reasoning capability; (ii) exploring the optimal generation configuration unleashes the full potential of existing LVLMs, resulting in substantial performance improvements compared to default configurations; (iii) the debiasing methods rectify model predictions, particularly in situations where the model lacks confidence and is prone to errors; and (iv) we scrutinize the failure cases of our methods, revealing certain flaws in current evaluation benchmarks.

3.1 Datasets and baselines

The paper employs a comprehensive evaluation strategy, leveraging four distinct datasets to assess the proficiency of LVLMs. Firstly, the MMMU dataset, spanning six core disciplines, rigorously tests models on multimodal questions

extracted from college exams, quizzes, and textbooks, emphasizing advanced **perception and reasoning** [51]. Secondly, the MME dataset systematically evaluates **perception and cognition capabilities**, encompassing tasks like OCR, object recognition, and reasoning across diverse modalities and cognitive domains [11]. The subsets within MME, such as MME-OH and MME-AH, specifically target **object-level and attribute-level hallucination** assessments [21]. Additionally, MME-RE includes reasoning subsets like code reasoning, text translation, commonsense reasoning, and numerical calculation to gauge cognitive abilities. Thirdly, the POPE benchmark introduces a refined approach for evaluating **object hallucination** in LVLMs. This benchmark underscores balanced sampling settings and draws data from MSCOCO, A-OKVQA, and GQA datasets [26]. Lastly, the LLaVA-Bench dataset scrutinizes LVLMs’ adaptability to **challenging tasks and new domains** through 24 diverse images and 60 questions, assessing robustness to various prompts [31]. Comprehensive details on these datasets are provided in the appendix B.

Evaluation of LVLM Baselines: The effectiveness of the proposed method is evaluated across three contemporary LVLMs. Specifically, we apply our methodology to LLaVA-1.5 and InstructBLIP, both utilizing Vicuna 7B as their language decoder [9, 30]. Additionally, we assess Qwen-VL and Qwen-VL-Chat, constructed on the Qwen 7B backbone [3]. In addition to the LVLMs, we introduce two Supervised Fine-Tuning (SFT) baseline approaches. Firstly, LLaVA-SFT [43] serves as a benchmark for our comparison. This model is trained on a novel mixture of data, combining synthetic vision instruction tuning data [31] with existing high-quality human-annotated multi-modal data in a conversational format. Secondly, LLaVA-RLHF [43] is trained using a LLaVA-SFT-13b initialized reward model and leverages the FACT-RLHF algorithm on the mixed data. To ensure a robust comparison, we present averaged results calculated over three runs on all benchmarks. Due to unreported generation parameters of VCD [21] on some benchmarks, we report re-implemented scores on these benchmarks. For all contrastive decoding strategies, we utilize the same hyper-parameters ($\alpha = 1$, $\beta = 0.1$). We execute all experiments on a machine equipped with an AMD EPYC 7542 32-Core Processor and $8 \times$ Tesla-V100 (40G) instances. To ensure robustness and reliability, we repeat each experiment three times using different random seeds. It is noteworthy that, at the time of our experimentation, the previously employed GPT-4 API (gpt-4-0314), as utilized in established benchmarks [30, 43], has been deprecated. Consequently, we adopt the updated GPT-4 API (gpt-4-0613) and present the re-evaluated performance in this paper.

3.2 Systematic Evaluation

Impact of Post-hoc Debias and Debias Sampling Methods on LVLM Performance: We conduct a comprehensive analysis by combining various debiasing strategies, including both post-hoc debias methods and debias sampling strategies, to investigate their influence on LVLM truthfulness and reasoning abilities. The results obtained from the MME dataset are presented in Tab. 1. Our key observations can be summarized as follows: (1) Post-hoc debias methods

Table 1: Performance of Various Debiasing Strategies on the MME Benchmark. The notation “VCD (u/n)” indicates the application of the VCD decoding strategy with either the None (u) or Unk (n) post-hoc debias methods.

LLaVA-v1.5-7B								
Subsets	Naive	Post-Hoc Debias			VCD [21]	Debias Sampling		
		None	Unk	Both		VDD-None	VDD-Unk	Both
MME-OH	313.33	335.00	328.33	303.33	303.33	316.67	318.33	328.33
MME-AH	260.00	315.00	305.00	275.00	283.33	296.67	291.67	291.67
MME-RE	317.86	302.50	299.29	282.50	312.14	279.64	337.50	346.07
Overall	891.19	952.50	932.62	860.83	898.81	892.98	947.50	966.07
LLaVA-v1.5-13B								
Subsets	Naive	VCD [21]	Unk	VDD-Unk	Mixed Strategy			
					VCD (u)	VCD (n)	VDD-None (u)	VDD-None (n)
MME-OH	291.67	316.67	343.33	351.67	338.33	333.33	348.33	348.33
MME-AH	280.00	253.33	320.00	308.33	318.33	318.33	325.00	320.00
MME-RE	357.14	284.29	277.86	361.43	279.29	281.79	267.50	269.29
Overall	928.81	854.29	941.19	1021.43	935.95	933.45	940.83	937.62

significantly enhance model truthfulness by mitigating hallucination, with both None and Unk strategies exhibiting superior performance compared to the naive approach, particularly in mitigating object and attribute hallucination; (2) Debias sampling strategies strike a better balance, with VDD-None and VDD-Unk achieving competitive hallucination scores while consistently outperforming in reasoning scores; (3) Combining different post-hoc debiasing strategies (Both) does not yield significant benefits, whereas combining debias sampling strategies shows promising results; (4) Post-hoc debiasing methods operate independently from sampling methods such as VCD and our proposed debias sampling methods. For instance, VCD (u), which combines VCD sampling with Unk post-hoc debiasing, outperforms VCD alone. Notably, VCD exhibits subpar performance with the LLaVA-13B model, likely due to its sensitivity to image noise levels. In contrast, our model relies on text rather than images, resulting in both higher efficiency and robustness. Similar patterns can also be observed in other datasets such as POPE (see Fig. 6), where the proposed debiasing methods and sampling techniques consistently outperform the naive and other baseline methods. Additionally, we notice that employing image-based debiasing methods such as Noise/Zero does not consistently yield improvements. In our experiments, we observe a much larger variance and sensitivity to question type with such methods, further emphasizing the robustness of our image-free debiasing strategies.

Effect of Decoding Strategies on LVLM Performance: In Tab. 2 (left), we conduct a comprehensive assessment of the LLaVA-v1.5 model’s performance across three distinct datasets—POPE-MSCOCO (average F1 across three subsets), MME (total score across 3 evaluation subsets), and MMMU (average ACC across 36 subsets)—by employing various decoding strategies and settings. The “Default” column denotes the baseline performance using default sampling parameters, while the “Sampling” columns exhibit results obtained through diverse

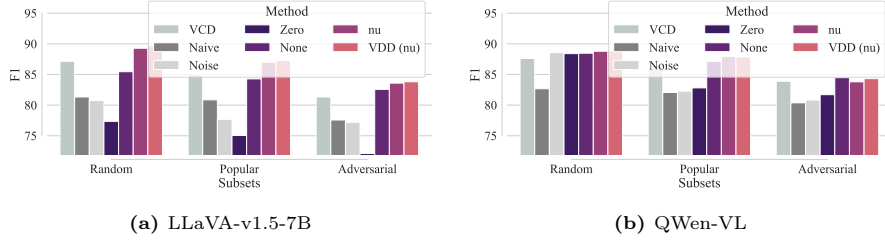


Fig. 6: Comparison of various post-hoc debiasing and sampling methods on the POPE-COCO benchmark. ‘nu’ denotes the application of both “None” and “Unk” for post-hoc debiasing, and “VDD-None” is used by default.

decoding strategies, including temperature (**Temp** τ), **Top- k** , and **Top- p** . The “Overall” column highlights the optimal performance achieved across all sampling strategies on all subsets. Notably, the application of the optimal sampling strategy leads to a substantial improvement in the overall model performance compared to default configurations. To underscore the generality of this phenomenon beyond LLaVA models, we extend our evaluation to include Qwen-VL and InstructBLIP in the POPE-MSCOCO benchmark. The results consistently demonstrate performance enhancements with refined sampling strategies across existing LVLMs. In Tab. 2 (right), we emphasize the superior performance of our proposed method, labeled as “Ours”, in comparison to alternative strategies. Our method surpasses fine-tuned models on specific instruction datasets, highlighting the effectiveness of our refined sampling strategies. Moreover, the 7B model, employing these refined sampling strategies, outperforms the 13B model with different fine-tuning strategies, including both supervised fine-tuning and RLHF. Additional detailed results for all subsets can be found in the appendix (Tabs. 6 and 8 to 10). Furthermore, a detailed comparison with additional baseline models on the POPE three subsets is provided in Tab. 11.

Overall Performance: Upon reaching the final iteration of our proposed method, we initially identify the optimal sampling configuration for all backbones. Subsequently, we apply debias sampling methods. Simultaneously, for classification tasks, we implement our post-hoc debiasing method, utilizing both None and Unk inputs concurrently. As depicted in Fig. 7, it becomes evident that VCD fails to consistently improve all baseline models, particularly in reasoning tasks. In contrast, our proposed method demonstrates superior results across all aspects and backbone models. Finally, the proposed method is assessed on the LLava-Bench, and the results presented in Fig. 8 demonstrate that, for open-ended generation tasks, VCD does not surpass the default decoding configuration consistently, although it occasionally outperforms in the complex subset. In contrast, our proposed VDD consistently exhibits improvements over the default decoding strategy. The right columns of the VDD section illustrate that, for generation tasks, model performance is consistently influenced by various decoding configurations. Unlike multi-choice QA tasks, which favor a low temperature

Table 2: Performance Evaluation of LLaVA-v1.5 with **Diverse Sampling Strategies (left)** and **Comparative Analysis with Baseline Models (right)** on the Adversarial Subset of the POPE Dataset. - means that the metric is not reported.

Dataset	Setting	Default		Sampling		Overall	Adversarial				
		LLaVA-v1.5		Temp	τ		Accuracy	Precision	Recall	F1	
POPE	7B	79.5	84.0	84.0	84.0	84.1	79.0	83.1	72.8	77.6	
	13B	77.2	84.2	84.2	84.1	84.2	67.2	-	-	74.7	
	Qwen-VL	81.8	83.6	83.7	83.3	83.7	82.3	-	-	81.1	
	InstructBLIP	78.9	79.8	84.5	79.9	84.5	82.3	-	-	80.5	
MSCOCO	7B	34.4	43.4	40.3	40.8	44.7	7B (Ours)	89.3	76.2	82.2	
	13B	36.3	43.2	43.4	43.1	45.8	13B (Ours)	91.6	75.6	82.8	
MMU	7B	313.3	363.3	345.0	355.0	363.3	Popular				
	13B	340.0	355.0	340.0	355.0	355.0	7B [21]	81.9	88.9	72.8	80.1
MME-OH	7B	260.0	323.3	301.7	325.0	330.0	13B [43]	73.6	-	-	78.2
	13B	303.3	321.7	311.7	321.7	321.7	SFT-13B [43]	84.0	-	-	82.6
MME-AH	7B	317.9	409.6	443.2	423.6	449.6	RLHF-13B [43]	83.9	-	-	81.8
	13B	295.4	428.9	405.7	415.0	453.9	7B (Ours)	85.9	94.3	76.3	84.4
MME-RE	7B	317.9	409.6	443.2	423.6	449.6	13B (Ours)	86.1	95.3	75.9	84.5
	13B	295.4	428.9	405.7	415.0	453.9					

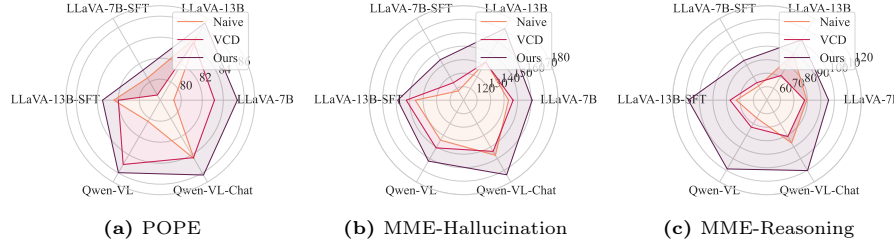


Fig. 7: Comparison with Baselines across Different Benchmarks and Varied Backbone Architectures. Detailed results are shown in Tab. 12-Tab. 15.

(τ), we observe that generation tasks benefit from a higher τ or a larger p value. Detailed results and results with larger backbones are shown in Tabs. 16 and 17. Qualitative examples in Appendix C.1 demonstrate that VDD is more helpful and less hallucinated, generating more precise illustrations.

3.3 Other Findings and Analysis

Calibration is particularly advantageous when a model lacks confidence in its predictions. In Figure 9, we analyze various post-hoc debiasing methods. It is evident that the 'Naive' approach performs poorly on instances where the model exhibits low confidence, which aligns with intuition. In contrast, our proposed post-hoc debiasing methods yield significant performance improvements for such cases. As prediction confidence increases, the model's predictions become more reliable and accurate, resulting in diminishing performance gains. Even at high confidence levels, around 0.9-1.0, our proposed methods achieve comparable results without detrimental effects. Consequently, the overall performance of our proposed method surpasses that of the naive

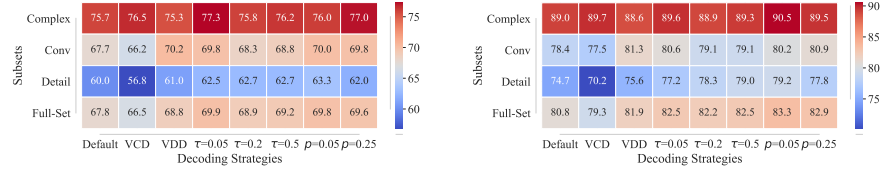


Fig. 8: Automatic evaluation of LLaVA-v1.5-7B on the LLaVA-Bench: GPT-4 compares model outputs with answers from GPT-4 (text-only) and assigns ratings in the range of [1, 10]. We present both absolute scores (left), scaled up to 100, and relative scores (right) compared to GPT-4 (text-only).

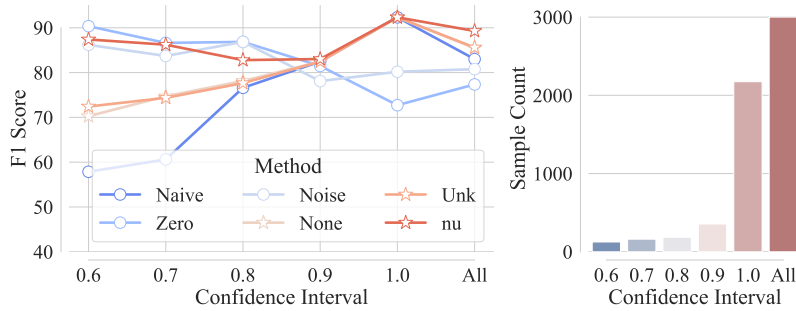


Fig. 9: Comparing the Effectiveness of Post-hoc Debiasing Methods Across Various Confidence Intervals. Here, 0.6 refers to instances with confidence ranging from 0.5 to 0.6, while other intervals exhibit similar characteristics.

approach. Notably, both image-based debiasing methods demonstrate superior performance on instances with low confidence scores, indicating aggressive adjustments to prediction results. However, such aggressive adjustments may lead to poorer predictions for high-confidence samples. Therefore, we default to using image-free debiasing methods, as they consistently yield improvements.

Navigating Challenges in Debiasing LLM-Biased Benchmarks: As illustrated in Fig. 10, we unravel the intricate interplay between debiasing methods and benchmarks influenced by LLM biases, with Naive’s performance centered around textual information. The post-hoc debiasing methods proposed exhibit inconsistent enhancements on the MMMU benchmark. Upon meticulous examination, when we entirely remove vision information by replacing the input image with an empty string (None*) or the <unk> identifier (Unk*), the model maintains comparable or superior performance in specific subsets. In these scenarios, our post-hoc methods, crafted to alleviate biases in LVLMs, fall short of yielding optimal results. Especially in instances where pure LLMs outshine, the application of post-hoc methods may prove detrimental. It is crucial to emphasize that benchmarks tailored for LVLMs should prioritize reliance on input images rather than solely on textual content. Consequently, our methods can act

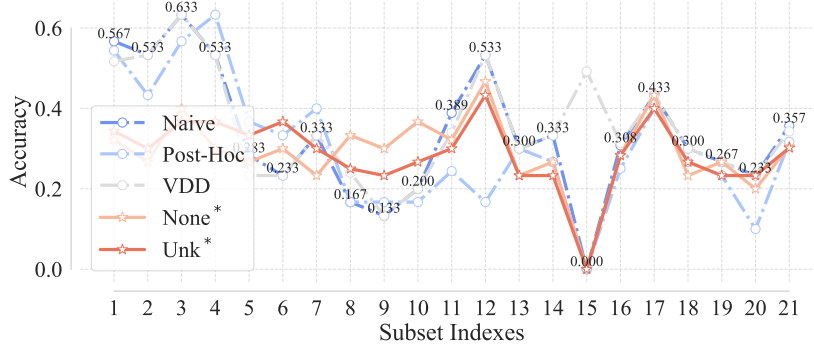


Fig. 10: Comparing Accuracy Across Subsets of the MMMU benchmark: the Naive and Post-Hoc debiasing methods leverage both vision and text information, while the None and Unk strategies replace the image with an empty string (‘’) and use the `<unk>` identifier, respectively, relying solely on textual information for evaluation. The accuracy of the Naive method is visually represented by the text.

as valuable indicators; when the proposed debiasing methods exhibit suboptimal performance, it signals that the benchmark may tilt more towards LLMs and may not be apt for evaluating LVLMs effectively. In such cases, the proposed sampling methods, VDD, also demonstrate inferiority compared to Naive, with an average accuracy of 34.3% versus 35.7%.

4 Concluding Remarks

We undertake a comprehensive exploration of biases and challenges associated with LVLMs, particularly focusing on their interaction with underlying LLMs. Our investigation exposes notable biases in LVLM-generated content, primarily influenced by the language priors ingrained in LLMs rather than the visual inputs. To address these biases, we introduce innovative debiasing strategies, including post-hoc debiasing methods and debias sampling techniques. Our experiments demonstrate the effectiveness of these strategies in mitigating hallucination and enhancing reasoning capabilities in LVLMs. Post-hoc debiasing methods, such as **None** and **Unk**, significantly improve model truthfulness, particularly when models lack confidence in their predictions. Moreover, debias sampling strategies, denoted as VDD, strike a balance by exhibiting competitive hallucination scores while consistently outperforming in reasoning tasks. The proposed strategies contribute to the reliability and applicability of LVLMs, addressing biases associated with language priors. Furthermore, our exploration into the impact of decoding configurations on LVLM performance reveals substantial improvements by refining sampling strategies. Optimal decoding configurations unleash the full potential of existing LVLMs, surpassing default configurations and raising concerns about the fairness of existing evaluations. As the field advances, addressing biases and refining evaluation methodologies are piv-

otal for harnessing the full potential of LVLMs in real-world applications. The **Limitations and Future Work** are shown in appendix D.

Potential Negative Impact. Exclusively prioritizing debiasing efforts may inadvertently introduce a conservative stance, potentially stifling the creative and exploratory facets of LVLMs. Striking a delicate balance between mitigating biases and preserving the generative potential is imperative to avoid constraining the model’s versatility. Additionally, the observed instability of LVLMs in response to decoding configurations underscores the potential for manipulation. Adversarial adjustments to decoding configurations could exploit this vulnerability, leading the model to generate harmful or realignment contents.

References

1. Anil, R., Dai, A.M., Firat, O., Johnson, M., Lepikhin, D., Passos, A., Shakeri, S., Taropa, E., Bailey, P., Chen, Z., et al.: Palm 2 technical report. arXiv preprint arXiv:2305.10403 (2023)
2. Awadalla, A., Gao, I., Gardner, J., Hessel, J., Hanafy, Y., Zhu, W., Marathe, K., Bitton, Y., Gadre, S., Sagawa, S., et al.: Openflamingo: An open-source framework for training large autoregressive vision-language models. arXiv preprint arXiv:2308.01390 (2023)
3. Bai, J., Bai, S., Yang, S., Wang, S., Tan, S., Wang, P., Lin, J., Zhou, C., Zhou, J.: Qwen-vl: A frontier large vision-language model with versatile abilities. arXiv preprint arXiv:2308.12966 (2023)
4. Brown, T., Mann, B., Ryder, N., Subbiah, M., Kaplan, J.D., Dhariwal, P., Neelakantan, A., Shyam, P., Sastry, G., Askell, A., et al.: Language models are few-shot learners. NeurIPS (2020)
5. Chen, H.T., Zhang, M., Choi, E.: Rich knowledge sources bring complex knowledge conflicts: Recalibrating models to reflect conflicting evidence. In: EMNLP (2022)
6. Chiang, W.L., Li, Z., Lin, Z., Sheng, Y., Wu, Z., Zhang, H., Zheng, L., Zhuang, S., Zhuang, Y., Gonzalez, J.E., et al.: Vicuna: An open-source chatbot impressing gpt-4 with 90%* chatgpt quality. See <https://vicuna.lmsys.org> (accessed 14 April 2023) (2023)
7. Chowdhery, A., Narang, S., Devlin, J., Bosma, M., Mishra, G., Roberts, A., Barham, P., Chung, H.W., Sutton, C., Gehrmann, S., et al.: Palm: Scaling language modeling with pathways. JMLR (2023)
8. Chuang, C.Y., Jampani, V., Li, Y., Torralba, A., Jegelka, S.: Debiasing vision-language models via biased prompts (2023)
9. Dai, W., Li, J., Li, D., Tiong, A., Zhao, J., Wang, W., Li, B., Fung, P., Hoi, S.: Instructblip: Towards general-purpose vision-language models with instruction tuning. arxiv 2023. arXiv preprint arXiv:2305.06500 (2023)
10. Driess, D., Xia, F., Sajjadi, M.S., Lynch, C., Chowdhery, A., Ichter, B., Wahid, A., Tompson, J., Vuong, Q., Yu, T., et al.: Palm-e: An embodied multimodal language model. arXiv preprint arXiv:2303.03378 (2023)
11. Fu, C., Chen, P., Shen, Y., Qin, Y., Zhang, M., Lin, X., Yang, J., Zheng, X., Li, K., Sun, X., Wu, Y., Ji, R.: Mme: A comprehensive evaluation benchmark for multimodal large language models. arXiv preprint arXiv:2306.13394 (2023)
12. Gao, P., Han, J., Zhang, R., Lin, Z., Geng, S., Zhou, A., Zhang, W., Lu, P., He, C., Yue, X., et al.: Llama-adapter v2: Parameter-efficient visual instruction model. arXiv preprint arXiv:2304.15010 (2023)

13. Gunjal, A., Yin, J., Bas, E.: Detecting and preventing hallucinations in large vision language models. arXiv preprint arXiv:2308.06394 (2023)
14. Guo, C., Pleiss, G., Sun, Y., Weinberger, K.Q.: On calibration of modern neural networks. In: ICML (2017)
15. Han, Y., Nie, L., Yin, J., Wu, J., Yan, Y.: Visual perturbation-aware collaborative learning for overcoming the language prior problem. arXiv preprint arXiv:2207.11850 (2022)
16. Hudson, D.A., Manning, C.D.: Gqa: A new dataset for real-world visual reasoning and compositional question answering. In: CVPR (2019)
17. Ji, Z., Lee, N., Frieske, R., Yu, T., Su, D., Xu, Y., Ishii, E., Bang, Y.J., Madotto, A., Fung, P.: Survey of hallucination in natural language generation. ACM Computing Surveys (2023)
18. Jiang, A.Q., Sablayrolles, A., Mensch, A., Bamford, C., Chaplot, D.S., Casas, D.d.l., Bressand, F., Lengyel, G., Lample, G., Saulnier, L., et al.: Mistral 7b. arXiv preprint arXiv:2310.06825 (2023)
19. Kim, J.M., Koepke, A., Schmid, C., Akata, Z.: Exposing and mitigating spurious correlations for cross-modal retrieval. In: CVPR (2023)
20. Laurençon, H., Saulnier, L., Tronchon, L., Bekman, S., Singh, A., Lozhkov, A., Wang, T., Karamcheti, S., Rush, A., Kiela, D., et al.: Obelics: An open web-scale filtered dataset of interleaved image-text documents. NeurIPS (2024)
21. Leng, S., Zhang, H., Chen, G., Li, X., Lu, S., Miao, C., Bing, L.: Mitigating object hallucinations in large vision-language models through visual contrastive decoding. arXiv preprint arXiv:2311.16922 (2023)
22. Li, B., Zhang, Y., Chen, L., Wang, J., Yang, J., Liu, Z.: Otter: A multi-modal model with in-context instruction tuning. arXiv preprint arXiv:2305.03726 (2023)
23. Li, C., Wong, C., Zhang, S., Usuyama, N., Liu, H., Yang, J., Naumann, T., Poon, H., Gao, J.: Llava-med: Training a large language-and-vision assistant for biomedicine in one day. arXiv preprint arXiv:2306.00890 (2023)
24. Li, J., Li, D., Savarese, S., Hoi, S.: Blip-2: Bootstrapping language-image pre-training with frozen image encoders and large language models. arXiv preprint arXiv:2301.12597 (2023)
25. Li, X.L., Holtzman, A., Fried, D., Liang, P., Eisner, J., Hashimoto, T., Zettlemoyer, L., Lewis, M.: Contrastive decoding: Open-ended text generation as optimization. arXiv preprint arXiv:2210.15097 (2022)
26. Li, Y., Du, Y., Zhou, K., Wang, J., Zhao, W.X., Wen, J.R.: Evaluating object hallucination in large vision-language models. arXiv preprint arXiv:2305.10355 (2023)
27. Liang, V.W., Zhang, Y., Kwon, Y., Yeung, S., Zou, J.Y.: Mind the gap: Understanding the modality gap in multi-modal contrastive representation learning. In: Koyejo, S., Mohamed, S., Agarwal, A., Belgrave, D., Cho, K., Oh, A. (eds.) NeurIPS (2022)
28. Lin, T.Y., Maire, M., Belongie, S., Hays, J., Perona, P., Ramanan, D., Dollár, P., Zitnick, C.L.: Microsoft coco: Common objects in context. In: ECCV (2024)
29. Liu, F., Lin, K., Li, L., Wang, J., Yacoob, Y., Wang, L.: Aligning large multi-modal model with robust instruction tuning. arXiv preprint arXiv:2306.14565 (2023)
30. Liu, H., Li, C., Li, Y., Lee, Y.J.: Improved baselines with visual instruction tuning (2023)
31. Liu, H., Li, C., Wu, Q., Lee, Y.J.: Visual instruction tuning. arXiv preprint arXiv:2304.08485 (2023)
32. Liu, H., Li, C., Wu, Q., Lee, Y.J.: Visual instruction tuning. NeurIPS **36** (2024)

33. Muennighoff, N., Wang, T., Sutawika, L., Roberts, A., Biderman, S., Scao, T.L., Bari, M.S., Shen, S., Yong, Z.X., Schoelkopf, H., et al.: Crosslingual generalization through multitask finetuning. arXiv preprint arXiv:2211.01786 (2022)
34. OpenAI.: Gpt-4 technical report (2023)
35. Phuong, M., Lampert, C.H.: Distillation-based training for multi-exit architectures. In: ICCV (2019)
36. Platt, J., et al.: Probabilistic outputs for support vector machines and comparisons to regularized likelihood methods. Advances in large margin classifiers (1999)
37. Radford, A., Kim, J.W., Hallacy, C., Ramesh, A., Goh, G., Agarwal, S., Sastry, G., Askell, A., Mishkin, P., Clark, J., Krueger, G., Sutskever, I.: Learning transferable visual models from natural language supervision (2021)
38. Rohrbach, A., Hendricks, L.A., Burns, K., Darrell, T., Saenko, K.: Object hallucination in image captioning. arXiv preprint arXiv:1809.02156 (2018)
39. Sahoo, D., Pham, Q., Lu, J., Hoi, S.C.: Online deep learning: Learning deep neural networks on the fly. arXiv preprint arXiv:1711.03705 (2017)
40. Schwenk, D., Khandelwal, A., Clark, C., Marino, K., Mottaghi, R.: A-okvqa: A benchmark for visual question answering using world knowledge. In: ECCV (2022)
41. Seth, A., Hemanu, M., Agarwal, C.: Dear: Debiasing vision-language models with additive residuals (2023)
42. Shi, W., Han, X., Lewis, M., Tsvetkov, Y., Zettlemoyer, L., Yih, S.W.t.: Trusting your evidence: Hallucinate less with context-aware decoding. arXiv preprint arXiv:2305.14739 (2023)
43. Sun, Z., Shen, S., Cao, S., Liu, H., Li, C., Shen, Y., Gan, C., Gui, L.Y., Wang, Y.X., Yang, Y., Keutzer, K., Darrell, T.: Aligning large multimodal models with factually augmented rlhf (2023)
44. Taori, R., Gulrajani, I., Zhang, T., Dubois, Y., Li, X., Guestrin, C., Liang, P., Hashimoto, T.B.: Stanford alpaca: An instruction-following llama model (2023)
45. Tonmoy, S., Zaman, S., Jain, V., Rani, A., Rawte, V., Chadha, A., Das, A.: A comprehensive survey of hallucination mitigation techniques in large language models. arXiv preprint arXiv:2401.01313 (2024)
46. Touvron, H., Lavril, T., Izacard, G., Martinet, X., Lachaux, M.A., Lacroix, T., Rozière, B., Goyal, N., Hambro, E., Azhar, F., et al.: Llama: Open and efficient foundation language models. arXiv preprint arXiv:2302.13971 (2023)
47. Touvron, H., Martin, L., Stone, K., Albert, P., Almahairi, A., Babaei, Y., Bashlykov, N., Batra, S., Bhargava, P., Bhosale, S., et al.: Llama 2: Open foundation and fine-tuned chat models. arXiv preprint arXiv:2307.09288 (2023)
48. Wei, J., Tay, Y., Bommasani, R., Raffel, C., Zoph, B., Borgeaud, S., Yogatama, D., Bosma, M., Zhou, D., Metzler, D., et al.: Emergent abilities of large language models. arXiv preprint arXiv:2206.07682 (2022)
49. Ye, Q., Xu, H., Xu, G., Ye, J., Yan, M., Zhou, Y., Wang, J., Hu, A., Shi, P., Shi, Y., et al.:mplug-owl: Modularization empowers large language models with multimodality. arXiv preprint arXiv:2304.14178 (2023)
50. Yuan, H., Lu, K., Huang, F., Yuan, Z., Zhou, C.: Speculative contrastive decoding. arXiv preprint arXiv:2311.08981 (2023)
51. Yue, X., Ni, Y., Zhang, K., Zheng, T., Liu, R., Zhang, G., Stevens, S., Jiang, D., Ren, W., Sun, Y., Wei, C., Yu, B., Yuan, R., Sun, R., Yin, M., Zheng, B., Yang, Z., Liu, Y., Huang, W., Sun, H., Su, Y., Chen, W.: Mmmu: A massive multi-discipline multimodal understanding and reasoning benchmark for expert agi. arXiv preprint arXiv:2311.16502 (2023)
52. Zhao, Z., Wallace, E., Feng, S., Klein, D., Singh, S.: Calibrate before use: Improving few-shot performance of language models. In: ICML (2021)

53. Zhibo, R., Huizhen, W., Muhua, Z., Yichao, W., Tong, X., Jingbo, Z.: Overcoming language priors with counterfactual inference for visual question answering. In: CCL (2023)
54. Zhou, W., Zhang, S., Poon, H., Chen, M.: Context-faithful prompting for large language models (2023)
55. Zhou, Y., Cui, C., Yoon, J., Zhang, L., Deng, Z., Finn, C., Bansal, M., Yao, H.: Analyzing and mitigating object hallucination in large vision-language models. arXiv preprint arXiv:2310.00754 (2023)
56. Zhu, D., Chen, J., Shen, X., Li, X., Elhoseiny, M.: Minigpt-4: Enhancing vision-language understanding with advanced large language models. arXiv preprint arXiv:2304.10592 (2023)
57. Zhu, X., Mao, Z., Liu, C., Zhang, P., Wang, B., Zhang, Y.: Overcoming language priors with self-supervised learning for visual question answering. arXiv preprint arXiv:2012.11528 (2020)

Debiasing Large Visual Language Models

Appendix

A Related Work

The landscape of **Large Vision-Language Models (LVLMs)** has undergone significant changes, initially rooted in BERT-based language decoders and later evolving to incorporate LLMs. LVLMs, heavily reliant on advanced LLMs like GPTs [4, 34], PaLM [1, 7], BLOOM [33], LLaMA [46, 47], Alpaca [44], Vicuna [6], and Mistral [18], exhibit enhanced capabilities and performance, particularly through end-to-end training techniques. Recent model developments, including Flamingo [2], PaLI [20], PaLM-E [10], BLIP-2 [24], InstructBLIP [32], Otter [22], MiniGPT-4 [56], mPLUG-Owl [49], LLaVA [23], and QWen-VL [3], bring unique perspectives to challenges such as scaling pre-training, enhancing instruction-following capabilities, and overcoming alignment issues between image and text modalities. However, it's crucial to note that while high-capability LLMs empower LVLMs, they also introduce biases, contributing to prevalent hallucination problems and generating unreliable content.

Hallucination in LVLMs is redefined from the NLP community's original concept of generating factual yet ungrounded content to encompass content not supported by the associated image [17, 45]. Several strategies have been explored to mitigate hallucinations in LVLMs. Initial efforts, geared towards small-scale VLMs, involved fine-grained modality alignment [38] and tackling statistical bias in object co-occurrence through data augmentation [19]. However, the distinctive behaviors of LVLMs pose a significant challenge, rendering existing methods impractical for generalization and scaling up [48]. Recent studies have addressed this challenge by introducing hallucination-targeted datasets for fine-tuning [13, 29], training a post-hoc revisor to generate less hallucinatory outputs [55], or adopting factually augmented Reinforcement Learning from Human Feedback (RLHF) [43]. While these interventions effectively address object hallucination in LVLMs, the associated human effort and computational costs underscore the need for a simpler yet efficient approach. A closely related method, VCD [21], manipulates the decoding distribution to reduce hallucination. In this paper, we demonstrate that VCD does not consistently bring improvement, and we propose a more efficient and effective method.

Addressing Biases in LVLMs. Recognizing the significant impact of language priors on Visual Question Answering (VQA) tasks [15, 53, 57], prior endeavors have primarily concentrated on bias mitigation within training sets. These initiatives entail the formulation of sophisticated training strategies and the construction of balanced datasets to tackle inherent biases. However, extending such methodologies LVLMs, which leverage pre-existing LLMs as text encoders, presents formidable challenges due to the intricate nature and resource-intensive process of retraining or fine-tuning. Moreover, the influence of language



Fig. 11: Selected Samples and Responses from LLaVA-v.15-7B. The visualization results for attention scores in (a) and (b) can be found in Figs. 5 and 12.

priors ingrained in utilized LLMs on LVLM performance remains uncertain. It is also noteworthy that certain works [8, 41] have delved into addressing biases in vision-language models. However, it is crucial to highlight that these works predominantly focus on social and group biases within vision-language models such as CLIP. Despite similarities in titles and overarching themes, their primary focus diverges substantially from our research objectives. Our investigation is uniquely centered on the nuanced biases inherent in LVLMs, providing a distinct perspective and contributions to the broader landscape of debiasing efforts in natural language understanding and computer vision.

B Dataset Details

Perception, Knowledge, and Reasoning: The MMMU dataset [51] consists of 11.5K meticulously collected multimodal questions sourced from college exams, quizzes, and textbooks. It spans six core disciplines (Art & Design, Business, Science, Health & Medicine, Humanities & Social Science, Tech & Engineering) and covers 30 subjects and 183 subfields. The dataset incorporates 30 highly

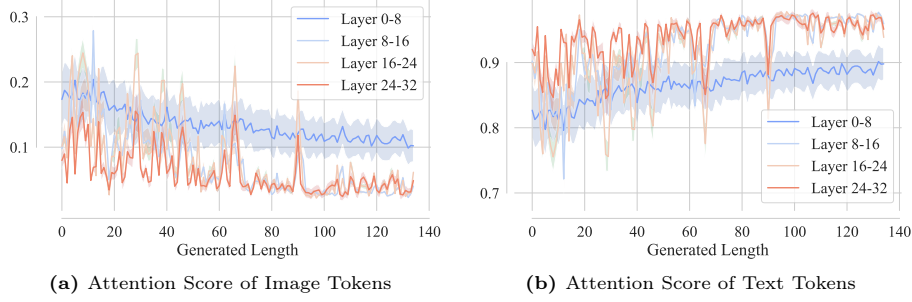


Fig. 12: Attention scores attained by each layer during generation.

diverse image types, including charts, diagrams, maps, tables, music sheets, and chemical structures. Unlike existing benchmarks, MMMU focuses on advanced perception and reasoning with domain-specific knowledge, challenging models to perform tasks similar to those encountered by experts.

Perception, Cognition, and Hallucination: The MME dataset [11] distinguishes itself by simultaneously appraising perception and cognition capabilities, encompassing tasks such as OCR, coarse-grained object recognition (encompassing existence, count, position, and color), and fine-grained object recognition (encompassing movie posters, celebrities, scenes, landmarks, and artworks). With a total of 14 subtasks, MME delivers a diverse and comprehensive evaluation, fulfilling the imperative for a thorough assessment of MLLMs across diverse modalities and cognitive domains. The existence and count subsets are applicable for object-level hallucination evaluation (**MME-OH**), while the position and color subsets are suitable for attribute-level hallucination (**MME-AH**) assessment [21]. Besides, we include four reasoning subsets: code reasoning, text translation, commonsense reasoning, and numerical calculation to evaluate the cognition ability (**MME-RE**).

Object Hallucination: POPE [26] introduces a streamlined method for evaluating object hallucination in Large Vision-Language Models (LVLMs). In this assessment framework, LVLMs are tasked with determining the presence of a specific object in a given image. The benchmark ensures a balanced ratio between queries probing existent and non-existent objects (i.e., 50% each). POPE incorporates three distinct sampling settings: random, popular, and adversarial, each creating negative samples in unique ways. In the random setting, objects absent from the image are chosen randomly, while the popular setting selects missing objects from a high-frequency pool. In the adversarial setting, priority is given to co-occurring objects not present in the image. The benchmark compiles data from three sources: MSCOCO [28], A-OKVQA [40], and GQA [16], utilizing 500 images from each dataset under each sampling setting. For each image, six questions are formulated, resulting in a total of 27,000 query-answer pairs from the development sets of these datasets. The evaluation focuses on four key metrics: Accuracy, Precision, Recall, and the F1 score.

Challenging Tasks and Generalizability to Novel Domains. LLaVA-Bench [31] is a dataset consisting of 24 images, spanning indoor and outdoor scenes, memes, paintings, and sketches, accompanied by a set of 60 questions designed to evaluate the capabilities of LVLMs. The dataset aims to assess the adaptability of LVLMs to challenging tasks and new domains. Each image is meticulously paired with a highly-detailed and manually-curated description, and questions are thoughtfully selected to encompass various contexts. Questions are categorized into conversation (simple QA), detailed description, and complex reasoning, aiming to evaluate the model’s robustness to diverse prompts.

C Extend experimental results

Table 3: COCO Object Categories

1. Person	21. Elephant	41. Wine Glass	61. Dining Table
2. Bicycle	22. Bear	42. Cup	62. Toilet
3. Car	23. Zebra	43. Fork	63. TV
4. Motorcycle	24. Giraffe	44. Knife	64. Laptop
5. Airplane	25. Backpack	45. Spoon	65. Mouse
6. Bus	26. Umbrella	46. Bowl	66. Remote
7. Train	27. Handbag	47. Banana	67. Keyboard
8. Truck	28. Tie	48. Apple	68. Cell Phone
9. Boat	29. Suitcase	49. Sandwich	69. Microwave
10. Traffic Light	30. Frisbee	50. Orange	70. Oven
11. Fire Hydrant	31. Skis	51. Broccoli	71. Toaster
12. Stop Sign	32. Snowboard	52. Carrot	72. Sink
13. Parking Meter	33. Sports Ball	53. Hot Dog	73. Refrigerator
14. Bench	34. Kite	54. Pizza	74. Book
15. Bird	35. Baseball Bat	55. Donut	75. Clock
16. Cat	36. Baseball Glove	56. Cake	76. Vase
17. Dog	37. Skateboard	57. Chair	77. Scissors
18. Horse	38. Surfboard	58. Couch	78. Teddy Bear
19. Sheep	39. Tennis Racket	59. Potted Plant	79. Hair Drier
20. Cow	40. Bottle	60. Bed	80. Toothbrush

C.1 Qualitative examples

We present examples in Fig. 15 to illustrate that the default decoding strategy leads to significant hallucinations in some instances, resulting in a low GPT-4 evaluation score (2). In these cases, VDD proves highly effective in alleviating hallucinations and achieving higher scores. A similar pattern is observed in

Fig. 16, indicating that merely scaling up the model cannot completely eliminate unrealistic patterns, while VDD consistently delivers superior performance. Examples in Fig. 17 further affirm the efficacy and accuracy of VDD, generating more precise illustrations.

D Limitations and Future Work

While our study represents a significant step forward in addressing biases and enhancing the performance of Large Vision-Language Models (LVLMs), it is essential to recognize certain limitations and outline promising avenues for future research.

Diversifying Evaluation Scenarios

Limitation: Our current evaluation primarily revolves around existing open-sourced LVLMs and datasets, focusing predominantly on QA and classification tasks.

Future Work: Expanding our evaluation scope to encompass a broader range of applications and scenarios, such as medical diagnostics, accessibility, and domain-specific use cases. This will provide a more comprehensive understanding of LVLM performance in diverse real-world contexts.

Attention Mechanism Enhancement

Limitation: The attention mechanism in LVLMs sometimes exhibits harmful patterns, emphasizing special tokens rather than crucial vision or text tokens. Our current method does not directly manipulate the attention mechanism.

Future Work: Investigating techniques to enhance the attention mechanism, redirecting focus towards vision tokens and key text tokens. This exploration aims to refine the model’s interpretability and ensure more meaningful attention during inference.

Innovative Fusion Techniques

Limitation: Current fusion strategies for combining vision and language modalities may benefit from further innovation to enhance overall LVLM performance.

Future Work: Exploring novel techniques for multimodal fusion, including innovative attention mechanisms and feature fusion strategies. These advancements aim to improve the synergy between vision and language representations, ultimately boosting the model’s overall effectiveness.

In conclusion, addressing these limitations and venturing into promising future research directions will play a pivotal role in advancing the field of Large Vision-Language Models. Continued collaboration and exploration across these dimensions will contribute to the development of more robust, interpretable, and versatile LVLMs for a wide array of applications.

Table 4: Identity-based Questions, the example identity is `cat`.

Number	What is the number of cats in the image?
Relation	What is the relation between the cat and the sofa in the image?
Color	What is the color of the cat in the image?
Action	What is the cat doing in the image?
Shape	What is the shape of the cat in the image?

Method	Decoding Configuration	Github Link
VCD	Default	https://github.com/DAMO-NLP-SG/VCD
LLaVA-v1.5	Greedy search	https://github.com/haotian-liu/LLaVA
InternLM	Beam (5) search	https://github.com/InternLM/InternLM-XComposer
PureMM	Greedy search	https://github.com/Q-MM/PureMM
INF-MLLM	Beam (5) search	https://github.com/infly-ai/INF-MLLM
LLaMA-Adapter	Top-p=0.75	https://github.com/OpenGVLab/LLaMA-Adapter
Otter	Default	https://github.com/Luodian/Otter
Qwen-VL	Top-p=0.01	https://github.com/QwenLM/Qwen-VL

Table 5: Decoding Configurations Across Various Models on the MME benchmark, Along with Access Links to Respective GitHub Pages for Detailed Information**Table 6: Performance of LLaVA-v1.5 with Various Sampling Strategies** on the POPE-MSCOCO benchmark . The default setting utilizes the performance reported in VCD [21], representing the most outstanding results observed to date.

LLaVA-v1.5-7B							InstructBLIP						
Subset	Default	Temp	τ	Top-p	Top-k	Overall	Subset	Default	Temp	τ	Top-p	Top-k	Overall
Adversarial	78.28	82.27	82.21	82.22	82.27	82.27	Adversarial	77.10	77.99	82.21	78.35	82.21	82.21
Popular	80.16	84.37	84.38	84.35	84.38	84.38	Popular	79.07	79.41	84.36	79.67	84.36	84.36
Random	80.00	85.49	85.51	85.51	85.51	85.51	Random	80.57	81.90	87.06	81.60	87.06	87.06
Average	79.48	84.05	84.03	84.03	84.05	84.05	Average	78.91	79.77	84.54	79.87	84.54	84.54
LLaVA-v1.5-13B							Qwen-VL						
Subset	Default	Temp	τ	Top-p	Top-k	Overall	Subset	Default	Temp	τ	Top-p	Top-k	Overall
Adversarial	74.74	82.84	82.82	82.75	82.84	82.84	Adversarial	80.68	82.25	82.41	82.10	82.41	82.41
Popular	78.80	84.44	84.50	84.41	84.50	84.50	Popular	81.80	84.11	84.10	83.68	84.11	84.11
Random	78.20	85.17	85.25	85.10	85.25	85.25	Random	82.82	84.53	84.44	84.21	84.53	84.53
Average	77.25	84.15	84.19	84.09	84.20	84.05	Average	81.76	83.63	83.65	83.33	83.68	83.68

Table 7: Performance of Various Debiasing Strategies on the MME Benchmark.

Subsets		Naive	LLaVA-v1.5-7B				Debias Sampling		
			None	Unk	Both	VCD [21]			
							VDD-None	VDD-UNK	Both
Object-level	existence	175.00	190.00	190.00	183.33	185.00	185.00	185.00	190.00
	Hallucination	138.33	145.00	138.33	120.00	118.33	131.67	133.33	138.33
Attribute-level	position	128.33	145.00	140.00	130.00	128.33	131.67	133.33	126.67
	Hallucination	131.67	170.00	165.00	145.00	155.00	165.00	158.33	165.00
Reasoning	commonsense	102.86	95.00	94.29	105.00	102.14	92.14	120.00	113.57
	numerical	60.00	70.00	67.50	45.00	92.50	70.00	77.50	70.00
	translation	92.50	50.00	50.00	47.50	70.00	72.50	92.50	75.00
	code	62.50	87.50	87.50	85.00	47.50	45.00	47.50	87.50
	MME-OH	313.33	335.00	328.33	303.33	303.33	316.67	318.33	328.33
MME-AH		260.00	315.00	305.00	275.00	283.33	296.67	291.67	291.67
Reasoning		317.86	302.50	299.29	282.50	312.14	279.64	337.50	346.07
LLaVA-v1.5-13B									
Subsets		Naive	Post-Hoc Debias				Debias Sampling		
			None	Unk	Both	VCD [21]			
							VDD-None	VDD-UNK	Both
Object-level	existence	180.00	188.33	188.33	190.00	173.33	190.00	188.33	190.00
	Hallucination	111.67	155.00	155.00	145.00	143.33	135.00	163.33	133.33
Attribute-level	position	130.00	165.00	165.00	155.00	123.33	138.33	143.33	143.33
	Hallucination	150.00	155.00	155.00	130.00	130.00	160.00	165.00	165.00
Reasoning	commonsense	112.14	115.00	112.86	122.14	134.29	115.71	116.43	111.43
	numerical	70.00	32.50	32.50	42.50	25.00	57.50	57.50	37.50
	translation	100.00	42.50	62.50	52.50	67.50	70.00	102.50	77.50
	code	75.00	70.00	70.00	52.50	57.50	62.50	85.00	60.00
	MME-OH	291.67	343.33	343.33	335.00	316.67	325.00	351.67	323.33
MME-AH		280.00	320.00	320.00	285.00	253.33	298.33	308.33	308.33
Reasoning		357.14	260.00	277.86	269.64	284.29	305.71	361.43	286.43

Table 8: Performance of LLaVA-v1.5 with Various Sampling Strategies on the MME benchmark. The default setting utilizes the default evaluation hyper-parameter [30].

LLaVA-v1.5-13B		Default	Temp	Top-k	Top-p	Overall
Object-level Hallucination	existence	185.0	195.0	185.0	195.0	195.0
	count	155.0	160.0	155.0	160.0	160.0
Attribute-level Hallucination	position	133.3	141.7	141.7	141.7	141.7
	color	170.0	180.0	170.0	180.0	180.0
Reasoning	commonsense-reasoning	127.9	136.4	125.7	135.0	136.4
	numerical-calculation	42.5	77.5	72.5	70.0	77.5
	text-translation	77.5	125.0	92.5	105.0	125.0
	code-reasoning	47.5	90.0	115.0	105.0	115.0
	All	938.7	1105.6	1057.4	1091.7	1130.6
LLaVA-v1.5-7B		Default	Temp	Top-k	Top-p	Overall
Object-level Hallucination	existence	175.0	195.0	190.0	195.0	195.0
	count	138.3	168.3	155.0	160.0	168.3
Attribute-level Hallucination	position	128.3	143.3	131.7	150.0	150.0
	color	131.7	180.0	170.0	175.0	180.0
Reasoning	commonsense-reasoning	102.9	122.1	120.7	113.6	122.1
	numerical-calculation	60.0	77.5	90.0	95.0	95.0
	text-translation	92.5	107.5	120.0	120.0	120.0
	code-reasoning	62.5	102.5	112.5	95.0	112.5
	All	891.2	1096.3	1089.9	1103.6	1143.0

Table 9: Performance of LLaVA-v1.5-7B with Various Sampling Strategies on the MMMU benchmark. The default setting utilizes the default evaluation hyper-parameter [30].

Subsets	Default	Temp	τ	Top- p	Top- k	Overall
Overall-Art and Design	0.517	0.533	0.517	0.533	0.533	
Art	0.533	0.600	0.567	0.567	0.600	
Art-Theory	0.633	0.700	0.633	0.667	0.700	
Design	0.533	0.600	0.633	0.600	0.633	
Music	0.367	0.400	0.400	0.433	0.433	
Overall-Business	0.240	0.293	0.267	0.260	0.293	
Accounting	0.200	0.400	0.333	0.333	0.400	
Economics	0.367	0.367	0.367	0.367	0.367	
Finance	0.100	0.300	0.267	0.200	0.300	
Manage	0.267	0.367	0.300	0.300	0.367	
Marketing	0.267	0.300	0.233	0.300	0.300	
Overall-Science	0.247	0.320	0.327	0.307	0.327	
Biology	0.133	0.333	0.267	0.267	0.333	
Chemistry	0.200	0.333	0.300	0.267	0.333	
Geography	0.400	0.467	0.467	0.467	0.467	
Math	0.267	0.467	0.367	0.400	0.467	
Physics	0.233	0.367	0.333	0.367	0.367	
Overall-Health and Medicine	0.333	0.360	0.367	0.347	0.367	
Basic-Medical-Science	0.533	0.567	0.533	0.533	0.567	
Clinical-Medicine	0.300	0.400	0.467	0.367	0.467	
Diagnostics-and-Laboratory-Medicine	0.333	0.433	0.433	0.367	0.433	
Pharmacy	0.367	0.500	0.367	0.400	0.500	
Public-Health	0.133	0.333	0.400	0.333	0.400	
Overall-Humanities and Social Science	0.492	0.533	0.500	0.508	0.533	
History	0.433	0.533	0.433	0.433	0.533	
Literature	0.767	0.800	0.767	0.800	0.800	
Sociology	0.400	0.500	0.433	0.433	0.500	
Psychology	0.367	0.467	0.467	0.500	0.500	
Overall-Tech and Engineering	0.314	0.329	0.319	0.333	0.333	
Agriculture	0.433	0.433	0.500	0.467	0.500	
Architecture-and-Engineering	0.400	0.400	0.300	0.333	0.400	
Computer-Science	0.200	0.300	0.300	0.367	0.367	
Electronics	0.233	0.333	0.233	0.333	0.333	
Energy-and-Power	0.400	0.500	0.400	0.400	0.500	
Materials	0.267	0.433	0.367	0.400	0.433	
Mechanical-Engineering	0.267	0.333	0.367	0.400	0.400	
Overall	0.344	0.434	0.404	0.408	0.447	

Table 10: Performance of LLaVA-v1.5-7B with Various Sampling Strategies on the MMMU benchmark. The default setting utilizes the default evaluation hyper-parameter [30].

Subsets	Default	Temp	τ	Top- p	Top- k	Overall
Overall-Art and Design	0.517	0.550	0.550	0.525	0.550	
Art	0.600	0.633	0.633	0.600	0.633	
Art-Theory	0.533	0.667	0.600	0.633	0.667	
Design	0.633	0.667	0.700	0.667	0.700	
Music	0.300	0.333	0.400	0.333	0.400	
Overall-Business	0.227	0.280	0.307	0.293	0.307	
Accounting	0.300	0.333	0.300	0.400	0.400	
Economics	0.233	0.400	0.433	0.367	0.433	
Finance	0.100	0.167	0.267	0.200	0.267	
Manage	0.333	0.400	0.333	0.400	0.400	
Marketing	0.167	0.300	0.333	0.300	0.333	
Overall-Science	0.287	0.307	0.307	0.327	0.327	
Biology	0.233	0.400	0.333	0.400	0.400	
Chemistry	0.167	0.267	0.267	0.267	0.267	
Geography	0.367	0.433	0.433	0.367	0.433	
Math	0.367	0.433	0.433	0.433	0.433	
Physics	0.300	0.300	0.367	0.500	0.500	
Overall-Health and Medicine	0.393	0.420	0.413	0.407	0.420	
Basic-Medical-Science	0.500	0.567	0.533	0.567	0.567	
Clinical-Medicine	0.433	0.467	0.467	0.467	0.467	
Diagnostics-and-Laboratory-Medicine	0.367	0.467	0.400	0.367	0.467	
Pharmacy	0.267	0.333	0.333	0.267	0.333	
Public-Health	0.400	0.467	0.533	0.433	0.533	
Overall-Humanities and Social Science	0.533	0.567	0.567	0.575	0.575	
History	0.567	0.600	0.633	0.600	0.633	
Literature	0.700	0.767	0.767	0.733	0.767	
Sociology	0.500	0.533	0.500	0.567	0.567	
Psychology	0.367	0.400	0.433	0.467	0.467	
Overall-Tech and Engineering	0.310	0.333	0.319	0.333	0.333	
Agriculture	0.500	0.600	0.567	0.533	0.600	
Architecture-and-Engineering	0.333	0.367	0.400	0.367	0.400	
Computer-Science	0.200	0.267	0.333	0.333	0.333	
Electronics	0.200	0.300	0.200	0.300	0.300	
Energy-and-Power	0.400	0.500	0.500	0.467	0.500	
Materials	0.367	0.433	0.433	0.467	0.467	
Mechanical-Engineering	0.167	0.300	0.300	0.267	0.300	
Overall	0.363	0.432	0.434	0.431	0.458	

Table 11: Performance Metrics on Adversarial, Popular, and Random Subsets of POPE-MSCOCO for Various Baseline Models. Reported performance is referenced for each model.

Model	Accuracy	Precision	Recall	Yes	F1
Adversarial					
LLaVA-v1.5-7B [21]	78.96	83.06	72.75	-	77.57
LLaVA-v1.5-7B [43]	62.70	-	-	83.00	72.00
LLaVA-v1.5-13B [43]	67.20	-	-	77.80	74.74
LLaVA-SFT+7B [43]	80.20	-	-	49.60	80.10
LLaVA-SFT+13B [43]	82.30	-	-	43.50	81.10
LLaVA-RLHF-7B [43]	80.70	-	-	44.00	79.50
LLaVA-RLHF-13B [43]	82.30	-	-	40.50	80.50
LLaVA-v1.5-7B (Ours)	83.52	89.25	76.22	42.70	82.22
LLaVA-v1.5-13B (Ours)	84.34	91.65	75.58	41.23	82.84
Popular					
LLaVA-v1.5-7B [21]	81.88	88.93	72.80	-	80.06
LLaVA-v1.5-7B [43]	68.40	-	-	77.90	75.30
LLaVA-v1.5-13B [43]	73.60	-	-	71.00	78.20
LLaVA-SFT+7B [43]	82.90	-	-	47.20	82.40
LLaVA-SFT+13B [43]	84.00	-	-	41.60	82.60
LLaVA-RLHF-7B [43]	83.30	-	-	41.80	81.80
LLaVA-RLHF-13B [43]	83.90	-	-	38.00	81.80
LLaVA-v1.5-7B (Ours)	85.87	94.32	76.33	40.47	84.38
LLaVA-v1.5-13B (Ours)	86.08	95.31	75.89	39.81	84.50
Random					
LLaVA-v1.5-7B [21]	83.29	92.13	72.80	-	81.33
LLaVA-v1.5-7B [43]	76.30	-	-	70.90	80.70
LLaVA-v1.5-13B [43]	73.70	-	-	72.30	78.80
LLaVA-SFT+7B [43]	86.10	-	-	45.50	85.50
LLaVA-SFT+13B [43]	82.30	-	-	43.50	81.10
LLaVA-RLHF-7B [43]	84.80	-	-	39.60	83.30
LLaVA-RLHF-13B [43]	85.20	-	-	38.40	83.50
LLaVA-v1.5-7B (Ours)	87.07	97.20	76.33	39.27	85.51
LLaVA-v1.5-13B (Ours)	86.88	97.29	75.87	38.99	85.25

Table 12: Performance Evaluation on POPE: 'Naive Decoding' signifies direct sampling, while 'VCD' denotes Vision Contrastive Decoding. 'Ours' refers to our proposed methods, incorporating the optimal sampling strategy. The most outstanding performances in each scenario are highlighted for clarity.

Dataset	Setting	Model	Decoding	Accuracy	Precision	Recall	F1 Score
MSCOCO	Random	LLaVA-7B	Naive	83.29	92.13	72.80	81.33
			VCD	87.73	91.42	83.28	87.16
			Ours	90.03	97.36	79.13	88.79
	Popular	Qwen-VL	Naive	84.73	95.61	72.81	82.67
			VCD	88.63	94.64	81.91	87.81
			Ours	89.20	92.55	85.27	88.80
	Adversarial	LLaVA-7B	Naive	81.88	88.93	72.80	80.06
			VCD	85.38	86.92	83.28	85.06
			Ours	88.57	94.32	79.33	87.00
A-OKVQA	Random	Qwen-VL	Naive	84.13	94.31	72.64	82.06
			VCD	87.12	91.49	81.85	86.40
			Ours	87.67	90.94	83.67	87.15
	Popular	LLaVA-7B	Naive	78.96	83.06	72.75	77.57
			VCD	80.88	79.45	83.29	81.33
			Ours	84.00	90.03	76.47	82.70
	Adversarial	Qwen-VL	Naive	82.26	89.97	72.61	80.37
			VCD	84.26	85.84	82.05	83.90
			Ours	85.23	89.06	80.33	84.61
GQA	Random	LLaVA-7B	Naive	83.45	87.24	78.36	82.56
			VCD	86.15	85.18	87.53	86.34
			Ours	88.13	93.27	82.20	88.24
	Popular	Qwen-VL	Naive	86.67	93.16	79.16	85.59
			VCD	89.22	90.77	87.32	89.01
			Ours	89.43	89.15	89.80	89.47
	Adversarial	LLaVA-7B	Naive	79.90	80.85	78.36	79.59
			VCD	81.85	78.60	87.53	82.82
			Ours	86.57	90.07	82.20	85.95
COCO	Random	Qwen-VL	Naive	85.56	90.44	79.53	84.63
			VCD	87.85	88.10	87.53	87.81
			Ours	88.47	87.02	88.07	88.54
	Popular	LLaVA-7B	Naive	74.04	72.08	78.49	75.15
			VCD	74.97	70.01	87.36	77.73
			Ours	80.23	79.09	82.20	80.61
	Adversarial	Qwen-VL	Naive	79.57	79.77	79.23	79.50
			VCD	81.27	77.79	87.53	82.38
			Ours	82.33	82.21	82.53	82.37
VQA	Random	LLaVA-7B	Naive	83.73	87.16	79.12	82.95
			VCD	86.65	84.85	89.24	86.99
			Ours	88.97	93.72	83.53	88.33
	Popular	Qwen-VL	Naive	80.97	88.07	71.64	79.01
			VCD	85.59	86.88	83.84	85.33
			Ours	87.37	85.50	90.00	87.69
	Adversarial	LLaVA-7B	Naive	78.17	77.64	79.12	78.37
			VCD	80.73	76.26	89.24	82.24
			Ours	85.13	87.37	82.07	84.68
Caption	Random	Qwen-VL	Naive	75.99	78.62	71.40	74.84
			VCD	81.83	80.45	84.09	82.23
			Ours	82.43	77.85	91.00	83.90
	Popular	LLaVA-7B	Naive	75.08	73.19	79.16	76.06
			VCD	76.09	70.83	88.75	78.78
			Ours	81.81	81.70	82.07	81.77
	Adversarial	Qwen-VL	Naive	75.46	77.92	71.07	74.33
			VCD	80.01	77.86	83.85	80.75
			Ours	78.80	73.35	90.00	81.21

Table 13: Performance Evaluation on POPE of supervise fine-tuned models. 'Naive Decoding' signifies direct sampling; 'VCD' denotes Vision Contrastive Decoding. 'Ours' refers to our proposed methods, incorporating the optimal sampling strategy. The most outstanding performances in each scenario are highlighted for clarity.

Dataset	Setting	Model	Decoding	Accuracy	Precision	Recall	F1 Score
MSCOCO	Random	LLaVA-v1.5-7B-SFT	Naive	85.70	91.87	78.33	84.56
			VCD	83.17	87.32	77.60	82.17
			Ours	86.63	90.37	82.00	85.98
	Popular	LLaVA-v1.5-13B-SFT	Naive	86.30	95.64	76.07	84.74
			VCD	85.80	93.80	76.67	84.37
			Ours	87.97	92.98	82.13	87.22
A-OKVQA	Random	LLaVA-v1.5-7B-SFT	Naive	82.60	85.64	78.33	81.82
			VCD	79.73	81.06	77.60	79.29
			Ours	83.23	84.79	79.93	82.82
	Popular	LLaVA-v1.5-13B-SFT	Naive	83.97	90.34	76.07	82.59
			VCD	83.9	89.63	76.67	82.64
			Ours	84.93	88.64	80.13	84.50
GQA	Adversarial	LLaVA-v1.5-7B-SFT	Naive	79.6	80.33	78.40	79.35
			VCD	76.73	77.47	77.47	76.90
			Ours	80.43	78.57	81.67	80.75
	Random	LLaVA-v1.5-13B-SFT	Naive	81.83	86.04	76.00	80.71
			VCD	81.07	84.06	76.67	80.20
			Ours	81.93	81.68	82.33	82.01
A-OKVQA	Random	LLaVA-v1.5-7B-SFT	Naive	84.33	85.03	83.33	84.18
			VCD	82.10	81.00	83.87	82.41
			Ours	84.40	84.54	84.20	84.37
	Popular	LLaVA-v1.5-13B-SFT	Naive	87.2	90.73	82.87	86.62
			VCD	85.90	88.06	83.07	85.49
			Ours	87.37	88.95	85.33	87.10
GQA	Popular	LLaVA-v1.5-7B-SFT	Naive	79.53	77.45	83.33	80.28
			VCD	76.57	73.32	83.53	78.10
			Ours	79.93	77.41	84.53	80.82
	Adversarial	LLaVA-v1.5-13B-SFT	Naive	83.77	84.39	82.87	83.62
			VCD	82.70	82.46	83.07	82.76
			Ours	83.67	82.58	85.33	83.93
A-OKVQA	Adversarial	LLaVA-v1.5-7B-SFT	Naive	71.83	67.86	83.33	74.81
			VCD	70.53	66.28	83.60	73.94
			Ours	72.60	68.25	84.53	75.52
	Random	LLaVA-v1.5-13B-SFT	Naive	76.97	74.12	82.87	78.25
			VCD	76.17	72.83	83.47	77.79
			Ours	76.80	72.89	85.33	78.62
GQA	Random	LLaVA-v1.5-7B-SFT	Naive	84.70	85.68	83.33	84.49
			VCD	82.93	82.50	83.60	83.05
			Ours	85.43	86.52	85.87	85.69
	Popular	LLaVA-v1.5-13B-SFT	Naive	86.07	88.70	82.67	85.58
			VCD	85.67	86.74	84.20	85.45
			Ours	86.50	87.89	84.67	86.26
GQA	Popular	LLaVA-v1.5-7B-SFT	Naive	77.40	74.49	83.33	78.67
			VCD	74.57	70.81	83.60	76.67
			Ours	78.53	75.44	84.87	79.87
	Adversarial	LLaVA-v1.5-13B-SFT	Naive	81.10	80.16	82.67	81.39
			VCD	80.20	77.96	84.20	80.96
			Ours	82.03	80.09	85.67	82.60
GQA	Adversarial	LLaVA-v1.5-7B-SFT	Naive	73.27	69.24	83.73	75.80
			VCD	71.40	67.06	84.13	74.63
			Ours	73.33	69.27	83.87	75.87
	Popular	LLaVA-v1.5-13B-SFT	Naive	77.23	74.56	82.67	78.41
			VCD	76.70	73.24	84.13	78.31
			Ours	79.24	77.67	74.10	79.24

Table 14: Performance Evaluation on POPE of Qwen-VL-Chat and LLaVA-v1.5-13B. 'Naive Decoding' signifies direct sampling, while 'VCD' denotes Vision Contrastive Decoding. 'Ours' refers to our proposed methods, incorporating the optimal sampling strategy. The most outstanding performances in each scenario are highlighted for clarity.

Dataset	Setting	Model	Decoding	Accuracy	Precision	Recall	F1 Score
MSCOCO	Random	LLaVA-v1.5-13B	Naive	86.80	97.42	75.60	85.14
			VCD	86.93	95.48	77.53	85.58
			Ours	89.20	95.72	82.07	88.37
	Popular	Qwen-VL-Chat	Naive	86.93	98.34	75.13	85.19
			VCD	87.23	96.89	76.93	85.77
			Ours	89.23	96.16	81.73	88.36
	Adversarial	LLaVA-v1.5-13B	Naive	86.10	95.70	75.60	84.47
			VCD	85.40	92.01	77.53	84.15
			Ours	87.63	92.35	82.07	86.90
A-OKVQA	Random	Qwen-VL-Chat	Naive	86.07	96.16	75.13	84.36
			VCD	86.37	94.97	76.8	84.92
			Ours	87.77	92.95	81.73	86.98
	Popular	LLaVA-v1.5-13B	Naive	84.23	91.51	75.47	82.72
			VCD	83.23	87.45	77.60	82.23
			Ours	84.97	87.07	82.13	84.53
	Adversarial	Qwen-VL-Chat	Naive	84.17	91.77	75.07	82.58
			VCD	83.73	89.41	76.53	82.47
			Ours	84.50	86.47	81.80	84.07
GQA	Random	LLaVA-v1.5-13B	Naive	88.77	93.89	82.93	88.07
			VCD	87.47	89.97	84.33	87.06
			Ours	89.10	90.81	87.00	88.87
	Popular	Qwen-VL-Chat	Naive	88.03	95.97	79.4	86.9
			VCD	88.20	94.63	81.00	87.28
			Ours	89.83	93.27	85.87	89.41
	Adversarial	LLaVA-v1.5-13B	Naive	86.70	89.69	82.93	86.18
			VCD	85.33	86.05	84.33	85.19
			Ours	88.00	88.78	87.00	87.88
A-OKVQA	Random	Qwen-VL-Chat	Naive	87.7	95.20	79.40	86.59
			VCD	87.63	93.19	81.20	86.78
			Ours	89.40	92.34	85.93	89.02
	Popular	LLaVA-v1.5-13B	Naive	80.17	78.58	82.93	80.70
			VCD	78.70	75.95	84.00	79.77
			Ours	80.20	76.58	87.00	81.46
	Adversarial	Qwen-VL-Chat	Naive	82.43	84.53	79.40	81.88
			VCD	82.07	82.59	81.27	81.92
			Ours	82.83	81.19	85.47	83.27
GQA	Random	LLaVA-v1.5-13B	Naive	89.53	93.73	84.73	89.01
			VCD	88.87	91.11	86.13	88.55
			Ours	89.80	91.46	87.80	89.59
	Popular	Qwen-VL-Chat	Naive	87.60	93.32	81.00	86.72
			VCD	87.03	91.42	81.73	86.31
			Ours	88.67	88.67	88.67	88.67
	Adversarial	LLaVA-v1.5-13B	Naive	86.40	87.66	84.73	86.17
			VCD	84.80	83.90	86.13	85.00
			Ours	87.50	87.28	87.80	87.54
A-OKVQA	Random	Qwen-VL-Chat	Naive	83.77	85.74	81.00	83.30
			VCD	82.03	82.44	81.40	81.92
			Ours	82.70	78.84	89.40	83.79
	Popular	LLaVA-v1.5-13B	Naive	82.23	80.70	84.73	82.67
			VCD	80.97	78.07	86.13	81.90
			Ours	82.47	79.34	87.80	83.35
	Adversarial	Qwen-VL-Chat	Naive	82.53	83.56	81.00	82.26
			VCD	81.53	81.58	81.47	81.52
			Ours	81.23	77.19	88.67	82.53

Table 15: Performance Evaluation on MME: ‘Naive’ signifies direct sampling, while ‘VCD’ denotes Vision Contrastive Decoding. ‘Ours’ refers to our proposed methods, incorporating the optimal sampling strategy. The most outstanding performances in each scenario are highlighted for clarity.

		Split	LLaVA-v1.5-7B			LLaVA-v1.5-13B		
			Naive	VCD	Ours	Naive	VCD	Ours
MME-OH	Existence		175.0	185.0	190.0	180.0	173.3	195.0
	Count		138.3	118.3	143.3	111.7	143.3	160.0
MME-AH	Position		128.3	128.3	145.0	130.0	123.3	150.0
	Color		131.7	155.0	165.0	150.0	130.0	180.0
MME-RE	Commonsense		102.9	102.1	112.9	112.1	134.3	129.3
	Numerical		60.0	92.5	57.5	70.0	25.0	90.0
	Translation		92.5	70.0	142.5	100.0	67.5	87.5
	Code		62.5	47.5	70.0	75.0	57.5	100.0
Overall			891.2	898.8	1026.2	928.8	854.3	1091.8
		Split	LLaVA-v1.5-7B-SFT			LLaVA-v1.5-13B-SFT		
			Naive	VCD	Ours	Naive	VCD	Ours
MME-OH	Existence		170.0	185.0	190.0	195.0	195.0	195.0
	Count		120.0	140.0	151.7	165.0	170.0	170.0
MME-AH	Position		66.7	60.0	96.7	86.7	81.7	101.7
	Color		115.0	115.0	140.0	136.7	163.3	168.3
MME-RE	Commonsense		121.4	120.0	128.6	125.7	119.3	132.9
	Numerical		25.0	25.0	55.0	37.5	57.5	97.5
	Translation		50.0	50.0	77.5	67.5	80.0	107.5
	Code		52.5	65.0	75.0	60.0	52.5	95.0
Overall			720.6	760.0	914.4	874.0	919.3	1067.9
		Split	Qwen-VL-7B			Qwen-VL-Chat		
			Naive	VCD	Ours	Naive	VCD	Ours
MME-OH	Existence		155.0	165.0	165.0	173.3	165.0	185.0
	Count		103.3	120.0	145.0	133.3	136.7	156.7
MME-AH	Position		143.3	133.3	148.3	151.7	143.3	168.3
	Color		175.0	185.0	190.0	170.0	170.0	185.0
MME-RE	Commonsense		105.7	105.0	132.9	106.4	104.3	125.7
	Numerical		60.0	57.5	77.5	45.0	37.5	62.5
	Translation		67.5	85.0	132.5	127.5	112.5	152.5
	Code		27.5	45.0	92.5	67.5	70.0	100.0
Overall			837.4	895.8	1083.7	974.8	939.3	1135.7

Table 16: Automatic Evaluation of LLaVA-v1.5-13B on the LLaVA-Bench: GPT-4 compares model outputs with answers from GPT-4 (text-only) and assigns ratings in the range of [1, 10]. We present both absolute scores scaled up to 100 and relative scores compared to GPT-4 (text-only). The most exceptional performances in each subset are highlighted for clarity, excluding the Overall category.

LLava-v1.5-13B Absolute Score										
Subsets	Default VCD [21]	VDD								Overall VDD
		Naive		$\tau=0.05$		$\tau=0.2$		$\tau=0.5$		
Complex	75.70	76.50	75.30	77.30	75.80	76.20	76.00	77.00	77.30	
Conv	67.70	66.20	70.20	69.80	68.30	68.80	70.00	69.80	70.20	
Detail	60.00	56.80	61.00	62.50	62.70	62.70	63.30	62.00	63.30	
Full-Set	67.80	66.50	68.80	69.90	68.90	69.20	69.80	69.60	70.27	

LLava-v1.5-13B Relative Score										
Subsets	Default VCD [21]	VDD								Overall VDD
		Naive		$\tau=0.05$		$\tau=0.2$		$\tau=0.5$		
Complex	89.00	89.70	88.60	89.60	88.90	89.30	90.50	89.50	90.50	
Conv	78.40	77.50	81.30	80.60	79.10	79.10	80.20	80.90	81.30	
Detail	74.70	70.20	75.60	77.20	78.30	79.00	79.20	77.80	79.20	
Full-Set	80.80	79.30	81.90	82.50	82.20	82.50	83.30	82.90	83.67	

Table 17: Automatic Evaluation of LLaVA-v1.5-7B on the LLaVA-Bench: GPT-4 compares model outputs with answers from GPT-4 (text-only) and assigns ratings in the range of [1, 10]. We present both absolute scores scaled up to 100 and relative scores compared to GPT-4 (text-only). The most exceptional performances in each subset are highlighted for clarity, excluding the Overall category.

LLava-v1.5-7B Absolute Score										
Subsets	Default VCD [21]	VDD								Overall VDD
		Naive		$\tau=0.05$		$\tau=0.2$		$\tau=0.5$		
Complex	75.70	76.50	75.30	77.30	75.80	76.20	76.00	77.00	77.30	
Conv	67.70	66.20	70.20	69.80	68.30	68.80	70.00	69.80	70.20	
Detail	60.00	56.80	61.00	62.50	62.70	62.70	63.30	62.00	63.30	
Full-Set	67.80	66.50	68.80	69.90	68.90	69.20	69.80	69.60	70.27	

LLava-v1.5-7B Relative Score										
Subsets	Default VCD [21]	VDD								Overall VDD
		Naive		$\tau=0.05$		$\tau=0.2$		$\tau=0.5$		
Complex	89	89.7	88.6	89.6	88.9	89.3	90.5	89.5	90.50	
Conv	78.4	77.5	81.3	80.6	79.1	79.1	80.2	80.9	81.30	
Detail	74.7	70.2	75.6	77.2	78.3	79	79.2	77.8	79.20	
Full-Set	80.8	79.3	81.9	82.5	82.2	82.5	83.3	82.9	83.67	

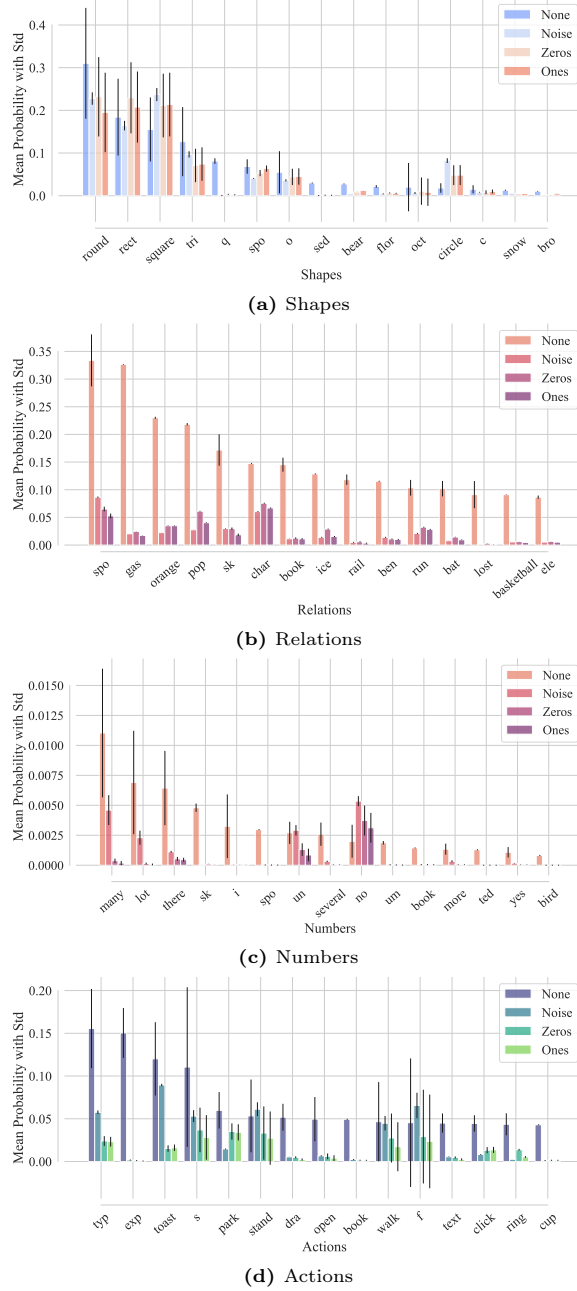


Fig. 13: Llava-v1.5-7B [30] model involves investigating biases across various scenarios. The term "None" indicates the absence of an input image, while "Noise" signifies the presence of Gaussian noise matching the image dimensions. "Zeros/ones" indicates a scenario where a tensor with all zero/one values aligning with the image shape is provided.

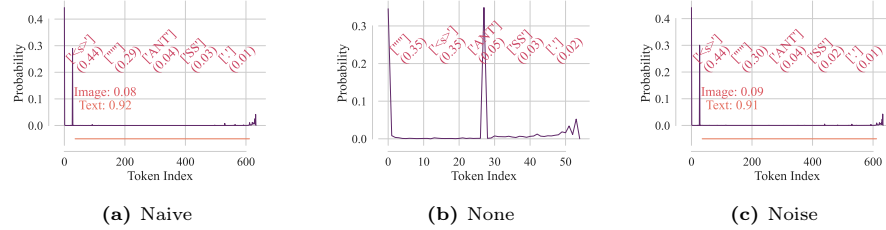


Fig. 14: Attention maps for different input images. The question is *A chat between a curious human and an artificial intelligence assistant. The assistant gives helpful, detailed, and polite answers to the human's questions. USER: <image> Is there a car in the image? Please answer this question with one word. ASSISTANT:*



Fig. 15: Qualitative examples showcasing the impact of VDD on LLaVA-v1.5-7B. VDD is demonstrated to be more helpful, minimizing hallucinations. For clarity, the hallucinated content is explicitly highlighted.

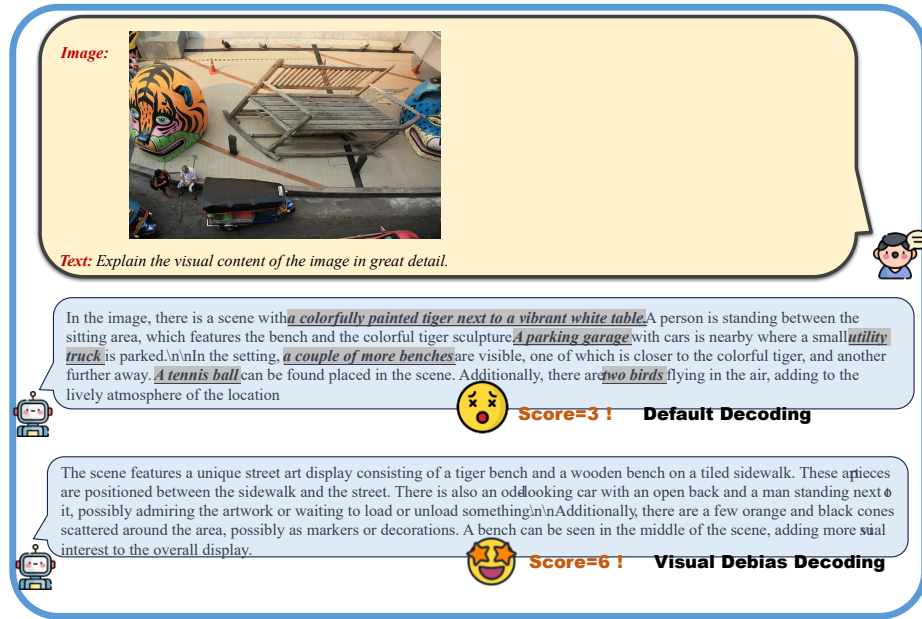


Fig. 16: Qualitative examples showcasing the impact of VDD on LLaVA-v1.5-13B. VDD is demonstrated to be more helpful, minimizing hallucinations. For clarity, the hallucinated content is explicitly highlighted.

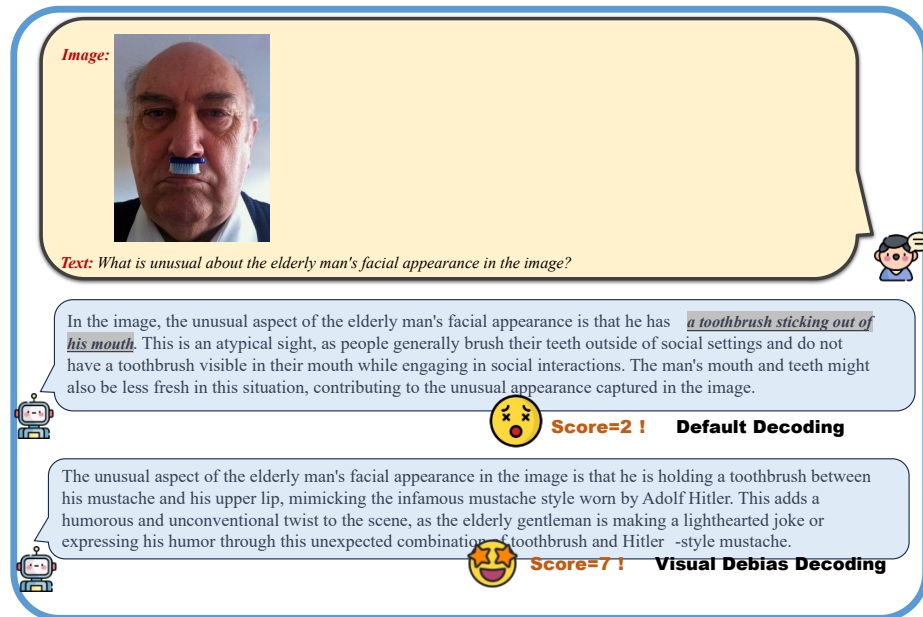


Fig. 17: Another Qualitative examples showcasing the impact of VDD on LLaVA-v1.5-13B. VDD is demonstrated to be more helpful, minimizing hallucinations. For clarity, the hallucinated content is explicitly highlighted.